Setting the dynein motor in motion: New insights from electron tomography

Published, Papers in Press, July 8, 2019, DOI 10.1074/jbc.REV119.003095

Danielle A. Grotjahn and Gabriel C. Lander[1]

From the Department of Integrative Structural and Computational Biology, The Scripps Research Institute, La Jolla, California 92037

Edited by Velia M. Fowler

Dyneins are ATP-fueled macromolecular machines that power all minus-end microtubule–based transport processes of molecular cargo within eukaryotic cells and play essential roles in a wide variety of cellular functions. These complex and fascinating motors have been the target of countless structural and biophysical studies. These investigations have elucidated the mechanism of ATP-driven force production and have helped unravel the conformational rearrangements associated with the dynein mechanochemical cycle. However, despite decades of research, it remains unknown how these molecular motions are harnessed to power massive cellular reorganization and what are the regulatory mechanisms that drive these processes. Recent advancements in electron tomography imaging have enabled researchers to visualize dynein motors in their transport environment with unprecedented detail and have led to exciting discoveries regarding dynein motor function and regulation. In this review, we will highlight how these recent structural studies have fundamentally propelled our understanding of the dynein motor and have revealed some unexpected, unifying mechanisms of regulation.

Dynein microtubule motor proteins are molecular engines responsible for a vast array of force-producing functions in eukaryotic cells, including intracellular transport, flagellar assembly, and cellular motility. The dynein superfamily is broadly divided into two main categories: axonemal dyneins and cytoplasmic dyneins. The cytoplasmic dyneins can be further categorized into intraflagellar transport (IFT)[2] dyneins and intracellular cytoplasmic dyneins (referred to hereafter as cytoplasmic dyneins), reflecting their involvement in disparate cellular functions. The importance of dynein motors is underscored by the plethora of human diseases associated with impairments to dynein function, including neurodegenerative diseases and ciliopathies (1–3).

All members of the dynein superfamily contain a large (over 4000 residues) subunit known as the dynein heavy chain. This massive polypeptide incorporates several conserved structural features that are fundamental to dynein function, the most salient of which is the AAA+ (ATPases associated with various cellular activities) motor. This multidomain structure harnesses the chemical energy of ATP hydrolysis to drive conformational rearrangements within the motor, giving rise to the unidirectional mechanical forces along microtubules that are used to perform a wide variety of cellular functions (Fig. 1). Although the motor domain has been extensively characterized through genetic, biochemical, and biophysical studies (4–20), the remaining portion of the dynein heavy chain, which is referred to as the tail domain, is much less characterized, partly because the tail is the most variable portion of the dynein heavy chain between different dynein subtypes. However, it has been established that the tail can facilitate dynein multimerization, and it serves as a platform for the association of dynein accessory subunits (21–23).

Despite the essential role that dynein plays in a diverse variety of cellular processes and the pathologies of several diseases, the precise molecular mechanisms responsible for dynein motility on microtubules, as well as the regulatory mechanisms that govern their spatiotemporal activity, remain largely unknown. Furthermore, although all dynein motors share a conserved motor domain, whether all members of the dynein superfamily operate by the same set of "rules" for achieving microtubule-based motility in their distinct subcellular environments and varying cellular functions remains unclear. Although the structural preservation of the motor domain indicates a conserved fundamental mechanochemical cycle (reviewed in Refs. 24–27), whether the conformational rearrangements are utilized for force production in the same manner across all dyneins remains an open question. Furthermore, it remains to be seen whether the dynein tail, which has become diversified through evolution to accommodate interaction with diverse components, retains functional and/or regulatory commonalities. Recent advances in EM have enabled researchers to begin probing such questions, such that unifying mechanistic principles that govern all forms of dyneins are beginning to emerge. Continued advances in specimen preparation, data acquisition, and image processing for *in situ* cryo-EM analyses provide an exciting avenue toward a complete mechanistic understanding of these fascinating cellular motors.

This work was supported by a Pew Scholarship in the Biomedical Sciences from the Pew Charitable Trust and by National Institutes of Health Grant DP2EB020402. The authors declare that they have no conflicts of interest with the contents of this article. The content is solely the responsibility of the authors and does not necessarily represent the official views of the National Institutes of Health.

[1] To whom correspondence should be addressed. Tel.: 858-784-8793; E-mail: glander@scripps.edu.

[2] The abbreviations used are: IFT, intraflagellar transport; BICD, BicaudalD; DDB, dynein–dynactin–BICD complex; DDH, dynein–dynactin–Hook3 complex; TIRF, total internal reflection fluorescence; DMT, doublet microtubule; CP, central pair; ODA, outer dynein arm; cryo-CLEM, cryo-correlative light and EM; AMPPNP, 5′-adenylyl-β,γ-imidodiphosphate.

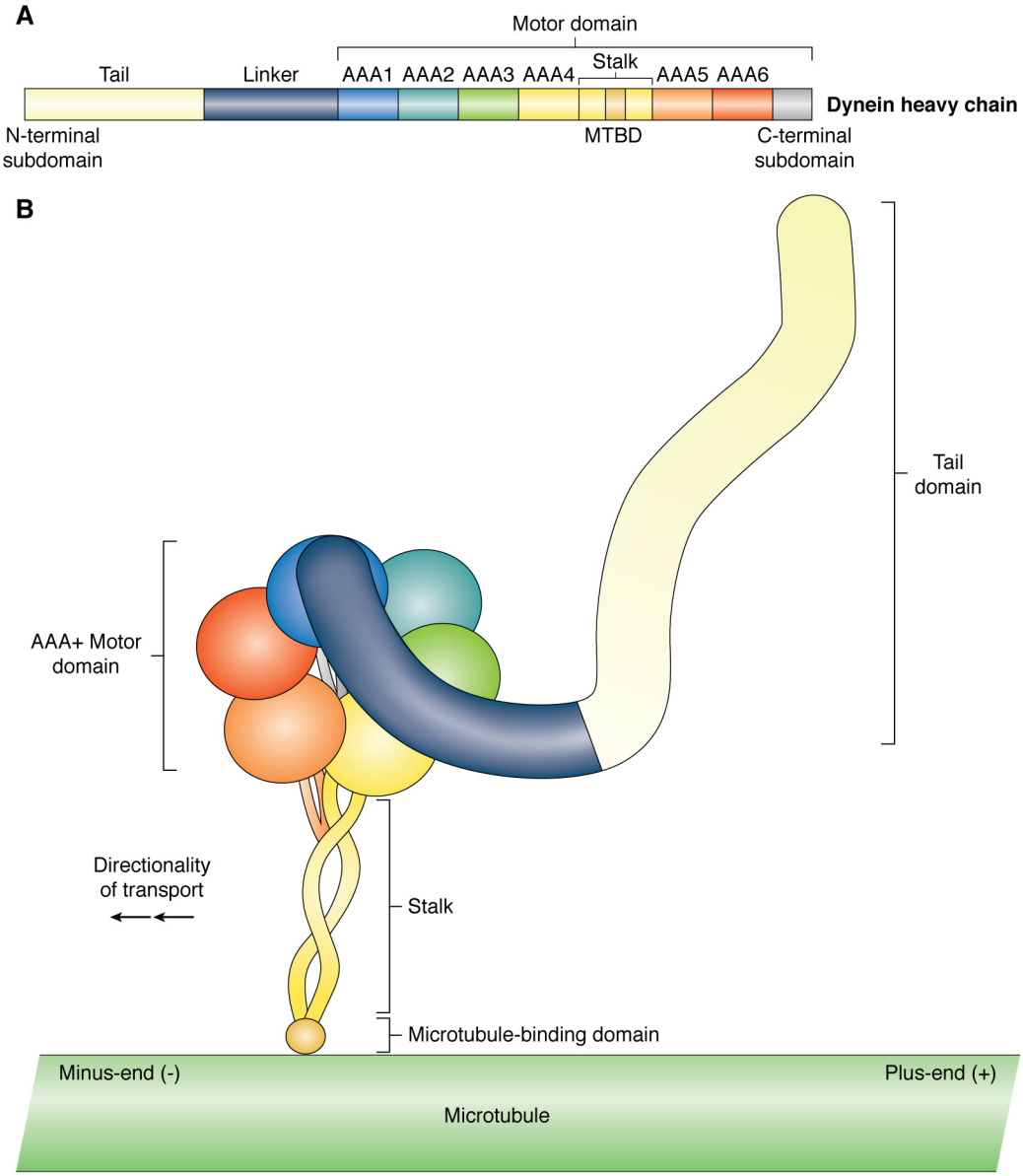

Figure 1. Domain architecture of the dynein heavy chain. *A,* schematic of the dynein heavy chain domain architecture with individual components colored and labeled, including the N-terminal tail, the linker, six AAA+ domains (*AAA1–AAA6*), stalk, microtubule-binding domain, and the C-terminal domain. *B,* cartoon representation of the dynein heavy chain bound to a microtubule (*green*) and oriented for transport toward the slow-growing, minus-end of the microtubule. Dynein heavy-chain domains are labeled and colored according to the schematic in *A*.

Dynein structure: a brief historical prospective

Structure-based techniques have been integral to the study of dynein motors since the initial discovery of dynein by Gibbons and Grimstone in 1960 (28) (Fig. 2), with the first fundamental insights into dynein motor composition arising from EM studies in which chemical fixation combined with deep-etch rotary shadowing or negative stain sample preparation procedures were used to generate two-dimensional snapshots of dynein molecules within their *in situ* or *in vitro* reconstituted transport environment (Fig. 2*A*) (29–36). These imaging modalities provided the necessary cellular *in situ* context to understand the overall architecture of dynein molecules (as indicated by *green stars* in Fig. 2) and demonstrated that all dynein motors share a common overall morphology, consisting of a flexible tail domain connected to a globular motor domain that terminates with a thin "stalk" that interacts with an associated microtubule (4, 31, 33, 34).

While these early studies greatly informed on the overall architecture of dyneins, the limited resolution of these techniques precluded detailed insights into the atomic-level mechanisms of microtubule-based motility (as indicated by *blue stars* in Fig. 2). Thus, researchers focused on purifying portions of the dynein molecule, leading to the first three-dimensional structures of the motor domain, revealing how the six concatenated AAA+ domains are organized into a ring-like structure (Fig. 2*B*) (5, 7, 8, 10, 14). Later, these robust purification strategies were also utilized in crystallographic studies to solve high-resolution structures of the dynein motor domain in the presence of different nucleotides, producing a burst of insights into the mechanochemical cycle of the dynein motor (Fig. 2*C*) (11–13,

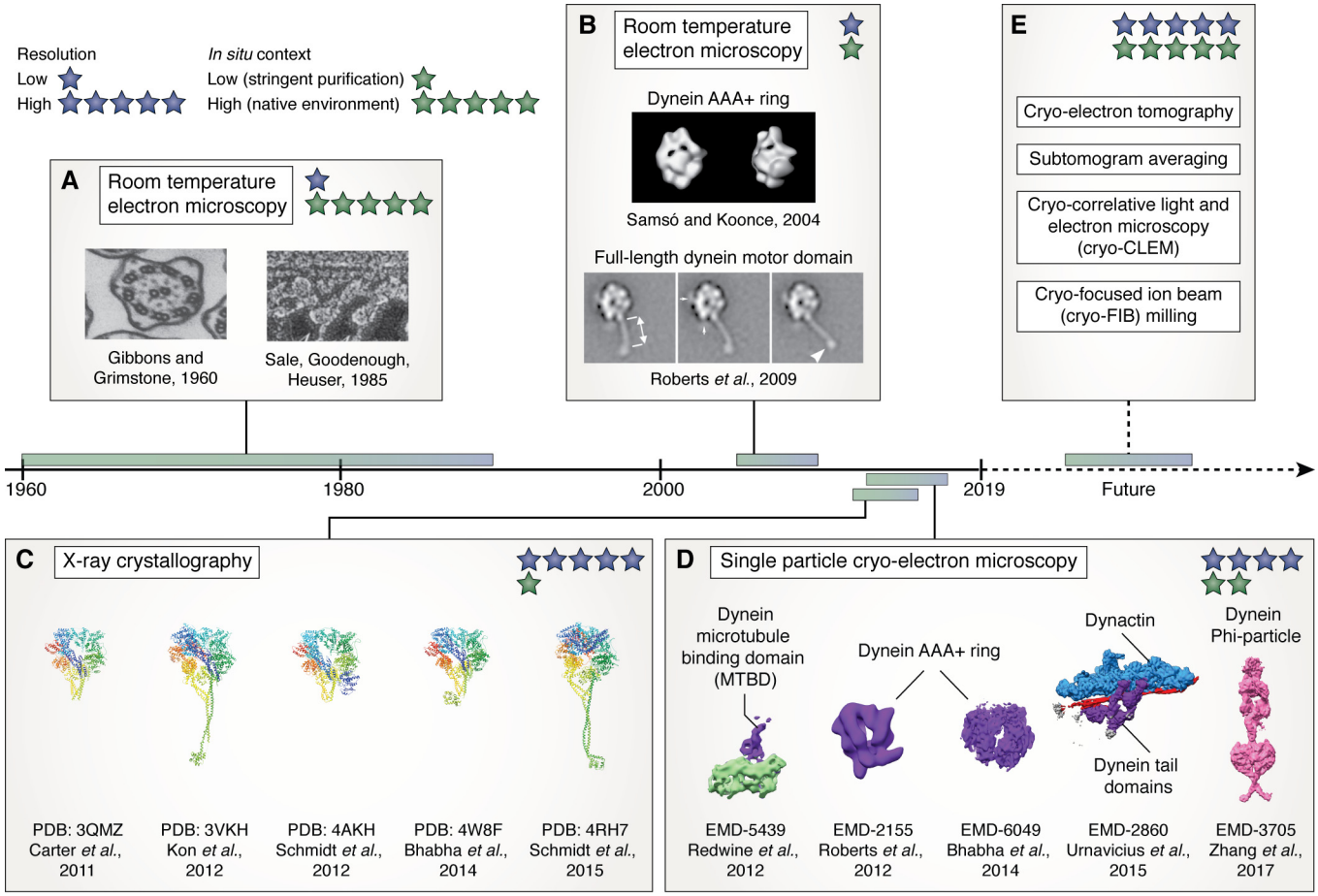

Figure 2. Timeline and representative images demonstrating the historical contribution of different structural techniques to the discovery and study of dynein motor proteins. *A,* from the 1960s to 1980s, low-resolution two-dimensional snapshots of dynein motors in their native cellular environment were captured using room temperature EM approaches. *B,* the application of advanced computational averaging techniques led to the first low-resolution, three-dimensional structures of the dynein heavy chain. *C,* later, crystallographic studies elucidated the precise atomic and large-scale rearrangements adopted by the dynein heavy chain at different stages of the mechanochemical cycle. *D,* recently, single particle cryo-EM approaches have resulted in three-dimensional structures of truncated portions of dynein heavy chain in association with their binding partners, including the microtubule-binding domain with tubulin subunit (EMD-5439), the dynein heavy chain tail with dynactin–cargo adaptors (EMD-2860), as well as full-length dynein in the inactive, ϕ-particle conformation (EMD-3705). *E,* in the future, dynein structure–function studies will likely depend on the combined application of cryo-electron tomography and subtomogram averaging with other advanced cellular imaging approaches such as cryo-CLEM and cryo-focused ion beam (*cryo-FIB*) milling. When utilized collectively, these approaches have the potential to be the preferred structural techniques capable of achieving high-resolution structures of dynein motors in their native, unperturbed cellular environment. Images from *A* were modified with permission from The Rockefeller University Press. Image in *B* was reprinted from Ref. 8 with permission from Elsevier.

16, 18, 20). Crystal structures of the motor domain in different conformational states showed how ATP binding and hydrolysis gave rise to large-scale rearrangements of the motor domain, with motions transmitted through the stalk to alter the binding affinity of the microtubule-binding domain.

Recently, advancements in the field of single particle room temperature and cryo-electron microscopy (cryo-EM) have enabled researchers to determine the high-resolution structures of larger multicomponent complexes that are recalcitrant to crystallization, providing structural details on several of the regulatory mechanisms of dynein function (Fig. 2*D*) (15, 17, 18, 37–39). Although advances in single particle cryo-EM are enabling the structure determination of increasingly larger and conformationally heterogeneous complexes, the extreme conformational heterogeneity of the flexible dynein complexes has impeded high-resolution single particle cryo-EM analyses of fully-assembled dynein motor protein complexes. Therefore, many unanswered questions regarding how these complexes are regulated to perform their essential cellular functions remain.

A related imaging technique called cryo-electron tomography (reviewed in Refs. 40, 41) occupies its own unique niche within the structural biology toolkit as the only technique capable of overcoming some of these fundamental challenges to structural visualization of dynein complexes, and it offers the exciting possibility to combine high-resolution structural analysis with cellular context, thereby bridging a fundamental gap within the dynein structural biology continuum (Fig. 2*E*). This imaging technique produces a three-dimensional volume, known as a tomogram, from a series of two-dimensional projection images generated by incremental tilting of the frozen-hydrated sample during imaging in a transmission electron microscope, thereby generating 3D representations of unique, heterogeneous cellular structures. Individual protein complexes present within the 3D tomograms can be computationally extracted and aligned using an image-processing technique

called subtomogram averaging to produce nanometer resolution, and even up to ~3 Å resolution (42) structures of protein complexes to reveal the 3D architecture of diverse macromolecules in action (reviewed in Ref. 43).

Tomography and subtomogram averaging approaches have been applied previously to visualize axonemal dynein motors, and the axonemal dynein field has benefited immensely from these structure–function studies. Over the past 15 years, the overall organization of the many axonemal dynein components and their regulatory cofactors has been mostly established (19, 44–49). Axonemal dynein is an ideal sample for cryo-electron tomographic approaches because a single flagellum or cilium can be readily purified, vitrified, tomographically imaged, and reconstructed. Furthermore, the presence of thousands of individual axonemal dynein motors within a single flagellum renders the sample ideal for subtomogram averaging to produce higher-resolution structures of axonemal dynein motors within their native environment. As a result, insights such as the complete ultrastructural organization of axonemal dynein subunits and a detailed powerstroke mechanism utilized by axonemal dynein motors to produce force on microtubules during ATP hydrolysis cycle have been proposed (19). However, there has been a notable lack of the same types of structure–function analysis of the other members of the dynein superfamily, and therefore, it is unclear whether the mechanistic insights gleaned from these studies on axonemal dynein motors can be applied to other members of the dynein superfamily. By recognizing structural similarities among the different dynein motors, we can develop testable hypotheses of dynein function and regulation, based on previously determined characteristics of axonemal dyneins (*i.e.* testing whether the powerstroke mechanism utilized by axonemal dyneins applies to cytoplasmic dyneins).

Within the past 2 years, cryo-electron tomography approaches have been applied to all members of the dynein superfamily, including the cytoplasmic and IFT dyneins, as groups have developed and utilized advanced tomography imaging and processing approaches to provide unprecedented views of dynein motors functioning in the context of their complex cellular microenvironment. Collectively, these structural analyses have led to paradigm-shifting views within the dynein motor field regarding the regulation and function of these fascinating motor proteins, and they provide compelling structural evidence that common mechanistic principles underlie the function of all dynein motors, despite their role in distinct cellular functions. This review provides an overview of these exciting recent studies and discusses how structures solved by electron tomography have revealed fundamental properties and commonalities that unite all members of the dynein motor protein family.

Tomographic characterization of three distinct dynein-based systems

Axonemal dyneins

Specialized, protruding, and membrane-bound organelles known as cilia are involved in several important functions such as cell signaling and cellular motility. These two distinct types of cilia are referred to as primary and secondary (or motile) cilia (also known as flagella), respectively. The fundamental core unit of both types of cilia is the axoneme, which comprises nine acetylated doublet microtubules arranged in a radial, ring-like pattern that emanates from a "basal body" organelle at the base of the flagellum. Reflective of their distinct functions, motile cilia or flagella (hereafter referred to simply as flagella) contain additional force-producing structures that power cell motility and fluid flow (Fig. 3*A*). These include a central pair of singlet microtubules that are connected to the radially distributed doublet microtubules through "radial spoke" proteins (Fig. 3*B*). Notably, thousands of individual dynein motors, collectively called axonemal dynein motors, line the microtubule doublets to establish a powerful inter-doublet network (29, 30, 32, 35, 50).

There are many distinct axonemal dynein isoforms whose activities are spatiotemporally regulated to differentially contribute to flagellar beating (51–54). However, these axonemal dyneins are generally categorized as inner-arm and outer-arm dyneins, reflecting their location relative to the central microtubule pair of microtubules within the axoneme (Fig. 3, *B* and *C*). Both categories of motors assemble into two distinct rows along the length of the axoneme such that their tail domain associates with the 13-protofilament A-tubule of one microtubule doublet, and their microtubule-binding domain associates with the 10-protofilament B-tubule of the adjacent doublet (Fig. 3, *B* and *C*). This cross-bridging pattern of dynein complexes across neighboring microtubule doublets is repeated throughout the length of the axoneme. Upon ATP hydrolysis, axonemal dyneins undergo conformational changes that produce a shear force on the B-tubule relative to the A-tubule, resulting in a sliding of adjacent microtubule doublets relative to one another (55–63). Decades ago, Wais-Steider and Satir (64) proposed a mechanism to explain how dynein-mediated microtubule sliding leads to the observed oscillatory, sinusoidal waveform (Fig. 3*A*) of beating of flagellum. The "switch point" mechanism proposed that the default conformation of axonemal dyneins was "inactive," and the activities of thousands of dyneins must be tightly regulated such that a bend is induced when a subset of dyneins restricted to a certain region of the axoneme become "active." A reversal in bend direction would require a "switch" in the population of dyneins that are "active" to the corresponding opposite side of the axoneme (64).

Recently, Lin and Nicastro (65) tested the switch-point hypothesis by using cryo-electron tomography to image the flagellum of a sea urchin sperm that had been actively swimming at the moment of vitrification. Although these tomograms contain a wealth of information regarding the conformational state of thousands of axonemal dyneins, the signal–to–noise is too low to elucidate the fine structural details of individual dynein molecules. Therefore, to determine the precise structural identity and position of distinct conformational states, the authors divided the tomograms of the undulating flagellum into smaller tomograms (sub-volumes), and they used a classification algorithm to sort and align axonemal dyneins exhibiting similar structural or conformational states into distinct 3D classes.

Lin and Nicastro (65) found that the majority of the axonemal dynein motors adopted a conformation wherein the AAA+ motor domain ring was rotated relative to the linker domain, and the microtubule-binding domain was detached

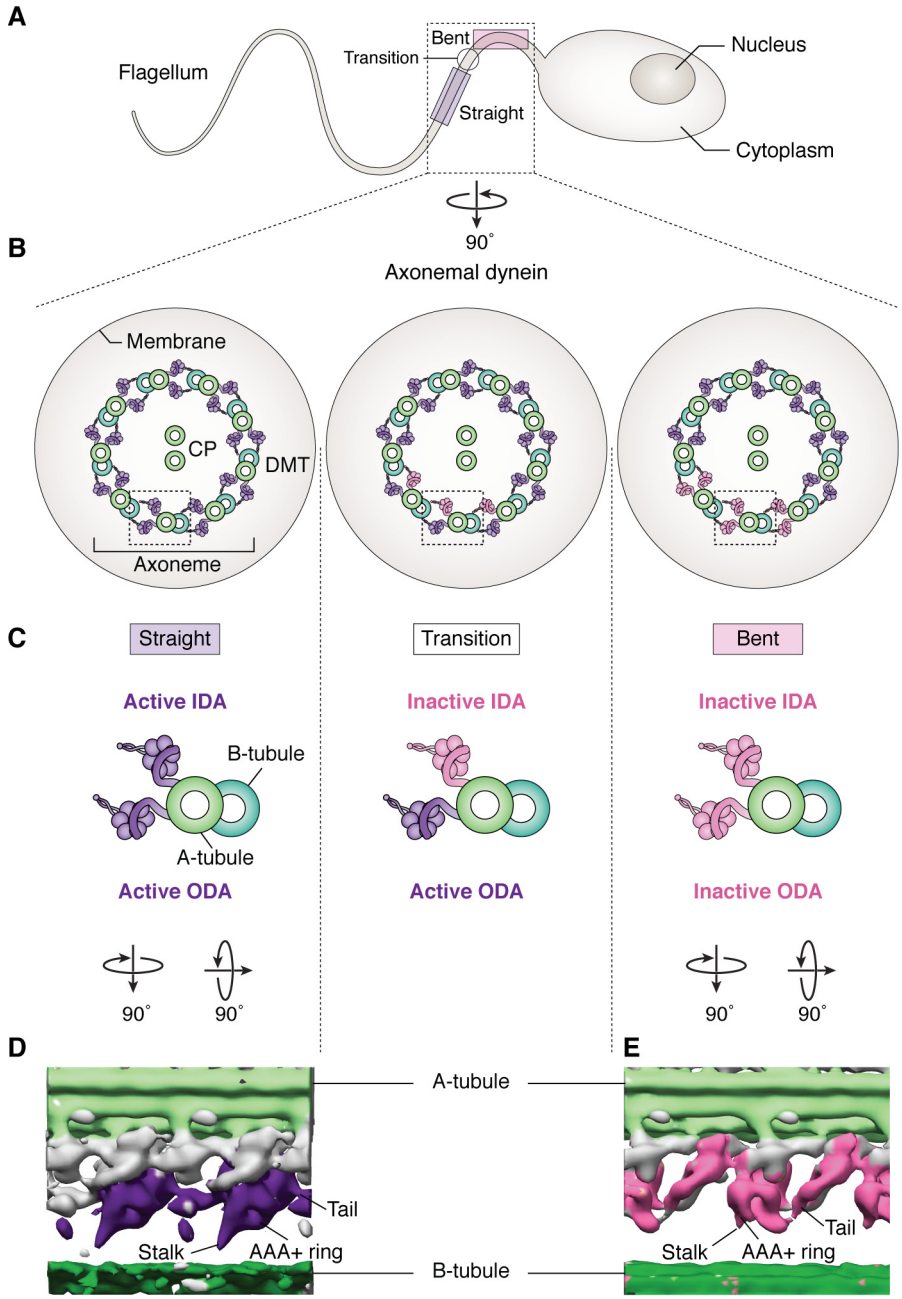

Figure 3. Axonemal dynein motors alter activity to induce oscillatory beating of motile flagellum. *A,* cartoon representation of a specialized eukaryotic cell containing a long flagellum used for cellular motility or fluid flow. *Colored box region* is expanded in *B–E*. *B,* axonemal dyneins within cross-sectional views of the flagellum labeled in *A* with labeled components of the axoneme, including DMT and the CP of microtubules. *Colored regions in the large box* correspond to the same portions of the flagellum depicted in *A*, including straight (*purple*), transition (*white*), and bent (*pink*) regions of the flagellum. *C, enlarged components of the boxed portions* displaying cross-sectional views of individual DMTs with attached outer dynein and inner dynein arms (labeled *ODA* and *IDA*, respectively) in their corresponding "active" (*purple*) or "inactive" (*pink*) states within the different straight, transition, and bent regions of the flagellum. *D,* subtomogram average structure (EMD-8836) of active ODAs (*purple*) found in straight regions of the flagellum. *E,* subtomogram average structure (EMD-8835) of inactive ODAs (*pink*) found in bent regions of the flagellum.

from the microtubule (Fig. 3*D*). The observed angle of the linker domain relative to the stalk domain was consistent with the "pre-power stroke" state previously described in high-resolution studies of the dynein motor (27). Because this dynein organization is representative of an ATP hydrolysis-competent motor that is "primed" for force-producing motions, the authors classify this conformation as an "active" state. The authors also identified a smaller subset (~6%) of dynein motors adopting conformations in which the microtubule binding domain was not resolved, but the motor domains were reminiscent of previously characterized "post-powerstroke" state (Fig. 3*E*). This indicated that these motors had completed the ATP hydrolysis cycle, including release of ADP and phosphate, leaving an unoccupied nucleotide-binding pocket within the AAA+ motor. The authors classify this conformation as an "inactive" state. Previous structural studies from Nicastro and co-workers (19) demonstrate that these diverse conformational states represent a direct readout of functional activity state (*i.e.*

active *versus* inactive) of dynein cycling through the force-producing mechanochemical cycle. However, it should be noted that the "inactive" state is not the same "ϕ-particle" inactive state that has been previously described for cytoplasmic dyneins (see below).

By mapping the location of subvolumes that comprise each 3D class to their original position within the 3D tomogram of the undulating flagellum, the authors revealed the conformational landscape and spatial distribution of "active" *versus* "inactive" axonemal dyneins relative to the positions of the sinusoidal axoneme. In contrast to previous switch-point dynein activation models, the authors unexpectedly discovered that the majority of outer-arm dyneins throughout the axoneme exhibit an "active" conformation (Fig. 3, *B–D*, *purple*), and only a small population of dyneins adopt "inactive" conformations (Fig. 3, *B, C,* and *E*, *pink*). The positions of these "inactive" dyneins correlate to the curvature of the sinusoidal flagellum, such that all microtubule doublets within the straight regions contain "active" dyneins, whereas the "inactive" dyneins are located on the inner concave side of the curved, beating flagellum (Fig. 3). Interestingly, within the "transition" zones, or regions of the flagellum that lie between straight and bent regions, all outer-arm dyneins adopt an "active" state, whereas a subset of the inner-arm dyneins are inactive (Fig. 3, *B* and *C*, *middle panel*). This suggests that an inhibitory signal may be primarily sensed by the inner-arm dyneins prior to the corresponding outer-arm dyneins as a means of initiating inactivation and subsequent flagellar bending (65). Collectively, these results defy the fundamental assumptions of the previously proposed "switch point" model of axonemal dynein regulation by demonstrating that the precise *inactivation,* rather than *activation*, of a subset of dynein molecules leads to the formation of a sinusoidal waveform that powers the motility of eukaryotic flagella. Future biochemical, structural, and functional assays are required to determine the precise identity and origin of the inhibitory signal that propagates along the length of the axoneme to regulate the dynein activity state during flagellar beating.

IFT dyneins

To sustain long-range eukaryotic cell motility, the assembly and upkeep of these specialized flagellar organelles are maintained in a process known as intraflagellar transport (IFT) (Fig. 4). The same microtubule doublets that harbor thousands of axonemal dyneins also serve as the roadways for cytoplasmic dynein-2 (referred to here as IFT dynein) and kinesin-II (IFT kinesin) motors, which assemble into large multiprotein assemblies called IFT "trains" that transport vital factors necessary for flagellar formation, maintenance, and function (Fig. 4, *B* and *C*) (36, 66–72)

In contrast to dynein motors, which move toward the structurally and chemically-distinct minus-end of the microtubule, kinesin proteins are microtubule plus-end–directed motors that move along the microtubule in the opposite direction (Fig. 4, *B* and *C*). This directional transport of molecular cargo by dynein and kinesin motors is called retrograde and anterograde transport, respectively. Notably, kinesin and dynein motors are structurally distinct, as kinesin motors contain a conserved G-protein domain fold in their motor domain, in contrast to the conserved AAA+ motor domain of dynein motors (25, 73). Reflective of these structural differences, kinesin motors utilize a "hand–over–hand" mechanism for microtubule-based transport that is fundamentally distinct from dynein (74, 75).

Axonemal microtubule doublets are oriented such that their minus-ends remain anchored to the basal body, and their plus-ends orient toward the distal tip, setting up an elegant transport system in which cellular cargoes necessary for flagellar elongations are transported away from the cellular cytoplasm by anterograde IFT kinesin-driven trains, and conversely, distal flagellar signals are propagated back by retrograde IFT dynein-driven trains (76–78). Interestingly, anterograde IFT trains contain both opposite-polarity IFT kinesin and dynein motors (79), yet they exhibit highly robust, efficient, and processive movement along the axoneme, without significant stalling, collision, or "tug–of–war" events, as defined by rapid, bidirectional reversals in the direction of motility (67, 80–82).

In 2016, Stepanek and Pigino (83) sought to investigate how this highly coordinated, dynamic transport behavior was achieved, and developed a novel, time-resolved correlative light and EM approach to investigate this system (84). This combinatorial approach took advantage of the two most powerful aspects of the respective imaging techniques: temporal resolution attained from total internal reflection fluorescence (TIRF) microscopy with spatial resolution provided by electron tomography (Fig. 2*E*). *Chlamydomonas* cells expressing GFP-labeled IFT trains within their highly elongated and projecting motile flagellum were immobilized within a specialized imaging chamber, and TIRF microscopy was used to generate kymographs that reported on the motility behavior of IFT trains before, during, and after cross-linking glutaraldehyde fixative is added to the imaging chamber, which effectively halted or arrested movement at a particular moment in time. Next, the same cell was imaged by electron tomography, thus yielding a detailed ultrastructural overview of the entire flagellum at the moment of fixation (72, 83, 85). By unambiguously mapping the positions of the IFT trains within the 3D tomogram back to their positions at the time of fixation within the TIRF kymographs, the authors discovered that all IFT trains moving in the anterograde direction immediately prior to fixation were associated with the B-tubule, and conversely, all retrograde IFT trains were consistently associated with the A-tubule (Fig. 4, *B–D*) (83). These results suggest that the mechanism by which IFT trains avoid collisions or "traffic jams" is through the utilization of structurally distinct tracks along the microtubule doublet during dynamic IFT. Although it still remains unclear how specificity for A-tubule *versus* B-tubules is achieved among IFT motors, it is possible that either the distinct geometry of the microtubule lattice or differential post-translational modifications (86–88) may contribute to selective structural and chemical preference of IFT kinesin and dynein motors (89, 90).

Although these results explained how collisions between anterograde and retrograde IFT trains are likely prevented, it remains unclear how IFT trains with bound IFT kinesin and dynein motors exhibit fast, directed movements that are devoid of "tug–of–war" motility properties (67, 81, 82). Negative stain EM structures of reconstituted IFT motor trains stably attached

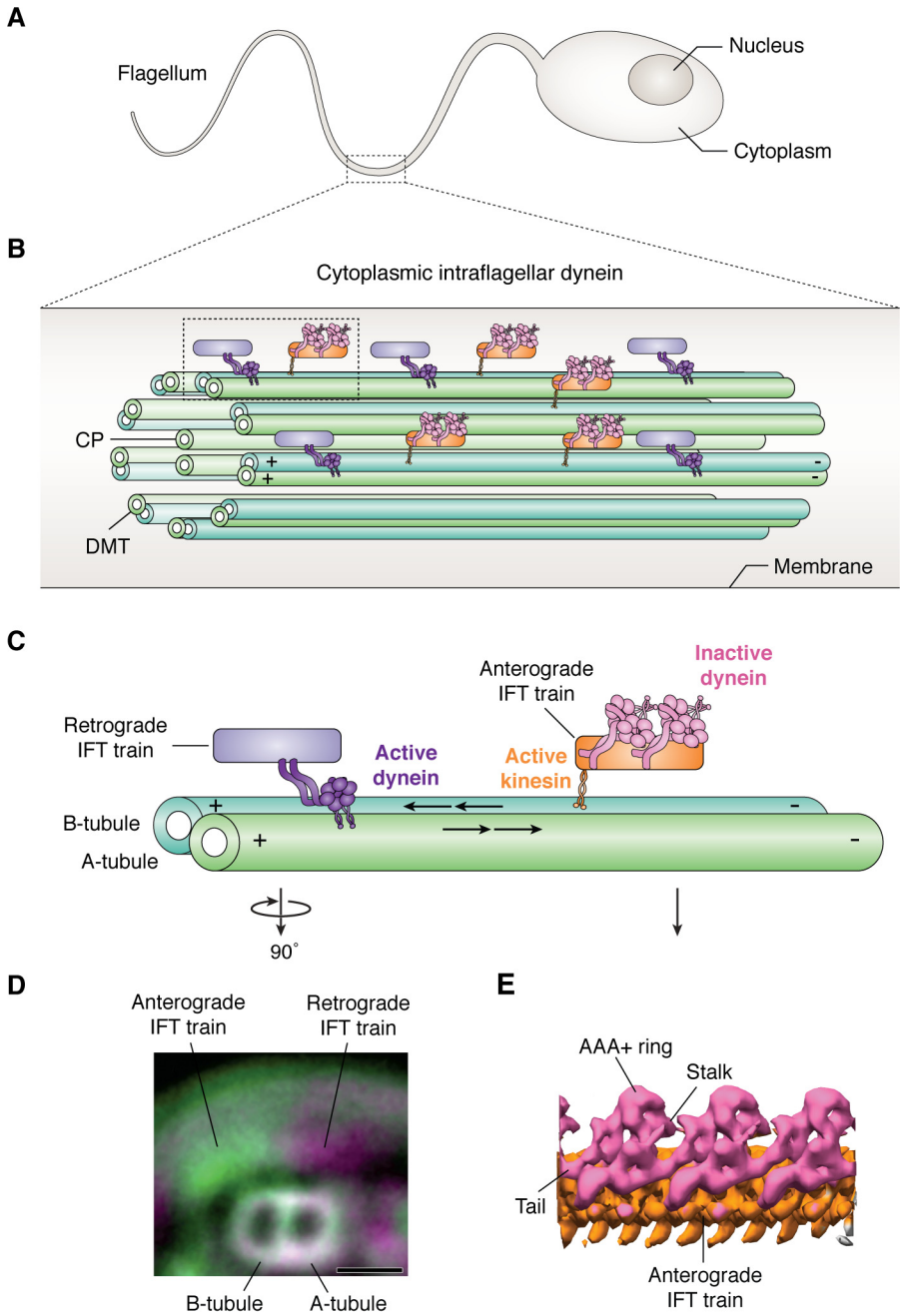

Figure 4. IFT dynein motors utilize multiple, distinct structural mechanisms to promote fast and efficient transport within eukaryotic flagellum. *A,* cartoon representation of a specialized eukaryotic cell containing a long flagellum used for cellular motility or fluid flow. *B,* cartoon representation of the IFT system within the membrane-bound flagellum labeled in the *boxed region* of *A* with labeled components of the axoneme, including the DMT and the CP of microtubules. *C, enlarged components of the boxed portion* showing retrograde IFT trains (*light purple*) containing active IFT dynein (*purple*), and anterograde IFT trains (*light orange*) containing active IFT kinesin (*orange*) and inactive IFT dynein (*pink*) transporting along the A- and B-tubule of the DMT, respectively. *D,* CLEM image from (83) of a cross-sectional view of a DMT showing preferential association of retrograde IFT trains (*purple*) and anterograde IFT trains (*green*) with the A- and B-tubule, respectively. *E,* subtomogram average structure (EMD-4303) of inactive IFT dynein motors (*pink*) bound to the anterograde IFT train (*orange*). Image in 4D is from Ref. 83. Reprinted with permission from AAAS.

to a DNA origami chassis revealed that, during anterograde IFT motility, IFT dynein motors adopt a conformation that resembles the previously-described, auto-inhibited "ϕ-particle" conformation (34, 39, 91, 92). In this conformation, the motor domains within the dynein homodimer are tightly stacked and rotated such that their respective linker domains contact one another, and the coiled-coil helices of the stalk are organized so that the microtubule-binding domain adopts a low-affinity state for the microtubule. Thus, by preventing microtubule association and subsequent translocation, these inactivated dynein motors become passive cargo on anterograde IFT trains, rather than opposing entities engaged in a tug-of-war with their kinesin counterparts. Recently, this model was confirmed *in situ* using a combination of cryo-electron tomography and subtomogram averaging approaches, demonstrating that IFT dynein motors adopt an auto-inhibited, ϕ-particle conformation with motor domains pointed toward the membrane in the direction opposite the corresponding B-tubule when associated

with anterograde IFT trains (Fig. 4, *B, C,* and *E*) (93). Collectively, these results suggest that the processive motility behavior of anterograde IFT trains is achieved through two distinct mechanisms to prevent association of IFT dynein with the microtubule: an auto-inhibitory conformation and a spatial positioning of the motor domains toward the membrane. Future work to determine the structural organization of active IFT dyneins during retrograde transport will ultimately reveal the entire conformational landscape of the IFT dynein and how these motors carry out their dynamic transport functions during flagellar formation and maintenance.

Intracellular cytoplasmic dyneins

Whereas axonemal and IFT dyneins utilize their force-producing capabilities to perform highly-specific and specialized tasks within a subset of flagellum-containing eukaryotic cells, metazoan intracellular cytoplasmic dynein (referred to here as cytoplasmic dynein) is responsible for the minus-end directed microtubule transport of nearly every type of molecular cargo within the intracellular transport network for all eukaryotic cells (Fig. 5). This includes the transport of mitochondria (94, 95), endosomes (96, 97), lysosomes (98), phagosomes (99), melanosomes (100, 101), peroxisomes (102), proteasomes (103), lipid droplets (104), viruses (105, 106), Golgi vesicles (107), centrosomes (108), transcription factors (109), neurofilaments (110), and mRNAs (111). In addition to its vital role during intracellular transport, cytoplasmic dynein is essential for successful completion of mitosis, as it functions to position the mitotic spindle apparatus, regulate the spindle assembly checkpoint, and promote the disassembly of the nuclear envelope (112, 113).

Unlike axonemal and IFT dyneins, which are readily identifiable within the confines of their flagellar microenvironment, accurately localizing individual cytoplasmic dynein molecules among the comparably larger and congested cytoplasmic landscape is extremely difficult using current imaging modalities, and to date the molecular ultrastructure of individual cytoplasmic dynein complexes has yet to be visualized *in situ*. This notable lack of structural information leaves many unanswered questions regarding the fundamental motile properties of cytoplasmic dynein, including the mechanisms by which cytoplasmic dynein is conformationally regulated to prevent wasteful ATP hydrolysis when dissociated from molecular cargo, and then subsequently activated for long-range (processive) microtubule-based transport of a wide variety of cellular cargo. Without a direct structural comparison, it is not possible to test whether some of the structure–function relationships that have been previously elucidated for the other dynein motors are relevant to or conserved in cytoplasmic dynein motors.

Nonetheless, to address some of these fundamental questions, previous studies have relied on complementary structural, biophysical, and biochemical approaches, as well as *in vitro* motility assays, to study purified cytoplasmic dynein motors within reconstituted transport environments. From these studies, it was demonstrated that isolated cytoplasmic dynein motors that are not attached to cargo can adopt an autoinhibited, ϕ-particle conformation similar to what is observed for IFT dyneins, wherein the motor domains adopt a stacked configuration to limit ATP hydrolysis, microtubule binding, and translocation (Fig. 5, *B–D*) (34, 39, 91) To initiate microtubule binding and subsequent translocation, it was shown previously that cytoplasmic dynein must be "activated" through the association of two additional cofactors—a large multisubunit complex named dynactin and any of a class of known "cargo adaptor" proteins (37, 38, 114, 115). The dynactin complex plays a well-established role in nearly every facet of cytoplasmic dynein function, including intracellular cargo transport and mitosis (116–122). Cargo adaptor proteins, however, were originally categorized as a group of coiled-coil proteins whose primary role was attaching dynein–dynactin complexes to the membrane of cellular cargo. For example, the cargo adaptor protein, bicaudalD, attaches dynein–dynactin complexes to the membrane of Rab6-containing vesicles (124–127), whereas Hook3 adaptor proteins connect dynein–dynactin to endosomal membranes (128, 129). Only within the past several years have *in vitro* motility assays shown that these cargo adaptors are not simply passive tethers between motors and cargo, but they appear to play a fundamental role in dynein activity, serving as molecular switches that conformationally induce highly robust, long-range or ultra-processive movement along microtubules (114, 115).

Despite these findings, the precise molecular details of this activation mechanism remained unclear due to a lack of structural information. Furthermore, in addition to mechanisms of processivity, another fundamental question regarding cytoplasmic dynein function centered on how a single isoform of the cytoplasmic dynein motor was able to accommodate the wide range of cellular cargoes associated with an enormous variety of cellular tasks, from large tubular mitochondria to small, packaged mRNAs. How this single motor could be fine-tuned to match the transport demands, including force-bearing load and transport velocity, of such diverse cargo remained an unsolved mystery.

To overcome some of these experimental challenges and to address these questions, our group developed a method to purify cytoplasmic dynein–dynactin–BICD (DDB) complexes stably bound to microtubules from mouse brain lysate in an effort to recapitulate a near-native transport environment (37), and our group performed cryo-electron tomography and subtomogram averaging to provide the first visualization of the 3D architecture of the entire intact microtubule-bound DDB complex (Fig. 5*E*) (130). Initially, the available subtomogram averaging strategies were unsuccessful in producing a 3D structure of this extremely heterogeneous, flexible motile complex sample, so we developed a guided subtomogram averaging approach, designed to facilitate the initial alignment of microtubule-bound DDB complexes, and further refined the structure using a series of 3D binary ellipsoid "masks" to help to restrict the alignment to smaller regions of the dynamic complex, thus producing well-aligned structures of portions of the complex that were combined to produce the final composite structure of the DDB–microtubule complex (Fig. 5*E*).

Surprisingly, our structure revealed the presence of two complete dimeric dynein densities bound to dynactin–BICD, with all four motor domains aligned longitudinally along adjacent protofilaments of the microtubule lattice (Fig. 5, *B, C,* and *E*).

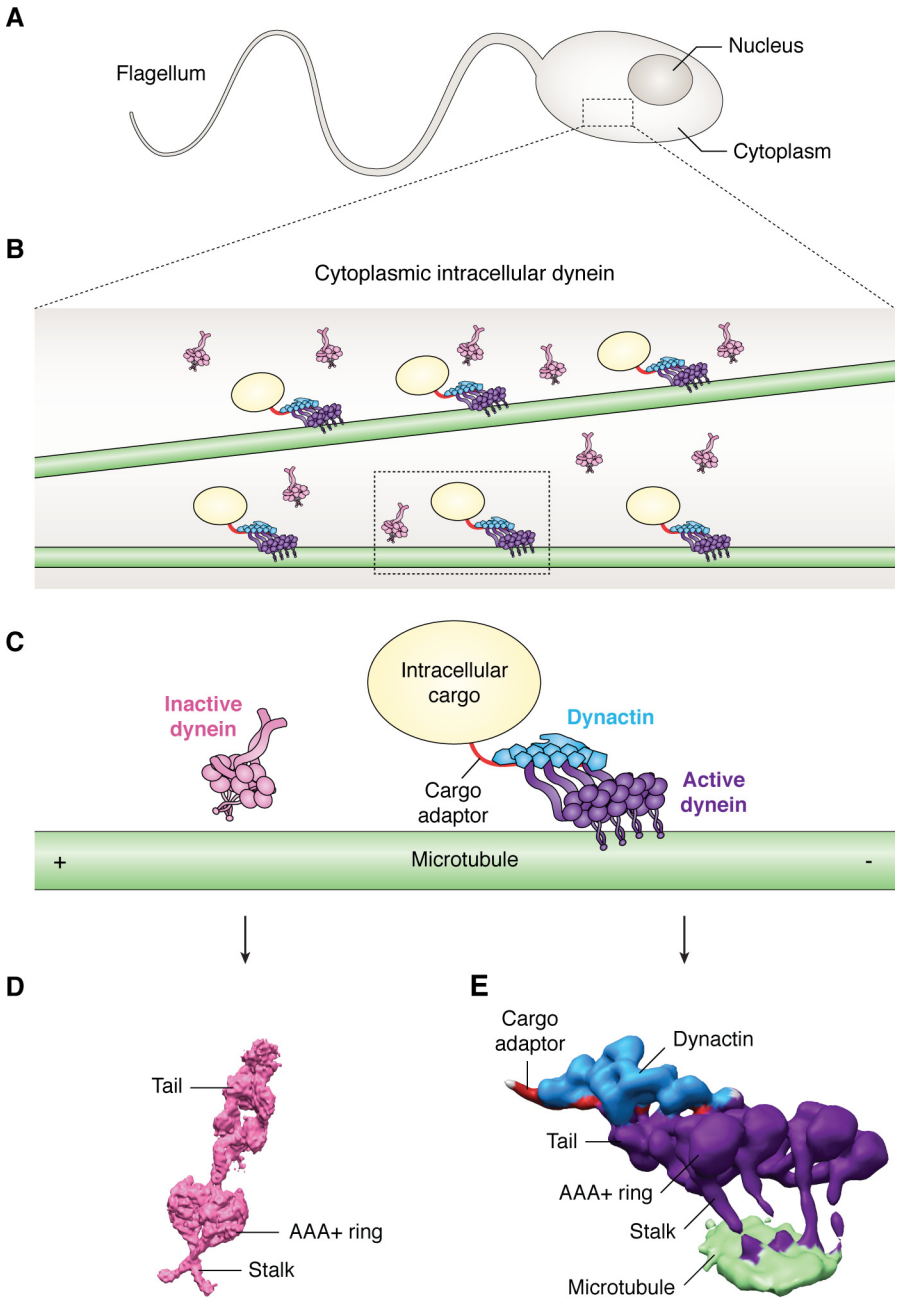

Figure 5. Cytoplasmic dynein motors can be recruited in pairs to dynactin–cargo adaptor complexes for processive, long-range transport of intracellular cargo. *A,* cartoon representation of a specialized eukaryotic cell containing a long flagellum used for cellular motility or fluid flow. It is worth nothing that, unlike the other members of the dynein family, cytoplasmic dyneins are present in all eukaryotic cells, including those cells that do not contain motile or primary cilia or flagella. *B,* cartoon representation of intracellular transport within the cytoplasm of the eukaryotic cell labeled in the *boxed region of A*. *C, enlarged components of the box* showing microtubule-detached, inactive cytoplasmic dynein (*pink*) alongside intracellular cargo (*yellow*) transported by two active cytoplasmic dynein complexes (*purple*) bound to a single dynactin (*cyan*)–cargo adaptor (*red*) complex. *D,* single particle structure (EMD-3705) of inactive cytoplasmic dynein (*pink*). *E,* subtomogram average structure (EMD-7000) of the active DDB complex bound to microtubules with individual components colored the same as in *B*.

This was unexpected because the DDB complex was previously characterized as containing one dynein molecule per dynactin–BICD (37, 38, 114, 115). To determine whether this 2:1 stoichiometry is specific to BICD or a conserved mechanism utilized by other processivity-inducing cargo adaptors, we performed similar purification, imaging, and data processing strategies to solve the first 3D structure of microtubule-bound dynein–dynactin–Hook3 complexes (DDH–microtubule) (130). Strikingly, the DDH–microtubule complex also contains two complete dimeric dynein complexes bound to dynactin–Hook3, suggesting that the recruitment of two complete dimeric cytoplasmic dynein molecules is a conserved mechanism utilized by dynactin and cargo adaptors to induce dynein activation and motility. Collectively, these results suggest that the dynactin–cargo adaptor complex serves as a stable "scaffold" to simultaneously attach multiple dynein complexes and stabilize or anchor dynein's otherwise flexible tail domains. Additionally, these structures suggested that spatially constraining the tail

domains through interactions with dynactin restricts the flexibility of the motor domains, such that they are more readily positioned for efficient, fast, and unidirectional motility on the microtubule surface. The presence of multiple motor domains within one dynactin–cargo–adaptor scaffold may reduce the probability of complex dissociation from the microtubule, as well as promote collective motor force production.

In agreement with these results, Carter and co-workers (131) used single particle cryo-EM to confirm the recruitment of two dynein tail domains to dynactin by cargo adaptors BICD2 and HOOK3. Interestingly, the authors showed with light microscopy that transport occurred in complexes containing a single dynein dimer, suggesting that there is some variability in the number of dynein molecules recruited to the dynactin–cargo adaptor complex. Although this is somewhat contradictory to our data that consistently (97%) showed two dyneins attached to the dynactin–cargo adaptor complexes, species-specific differences in the source of purified motor protein complexes, the presence of polymerized microtubules, and/or the use of the nonhydrolyzable ATP analog AMPPNP in our structural analysis may have promoted the recruitment of multiple dyneins to the dynactin–cargo adaptor complex. Collectively, these results suggest that there may be additional regulatory mechanisms that influence the stoichiometry of dynein bound to dynactin–cargo adaptor complexes. Intriguingly, Carter and co-workers (131) further demonstrated that the recruitment of a second dimeric cytoplasmic dynein complex leads to increased velocity and force production as compared with those complexes that recruit a single dynein dimer, suggesting that the dynein transport system may be fine-tunable depending on the type of cargo. This may also explain how a single cytoplasmic dynein isoform is able to transport a diverse array of cellular cargoes with differential velocities and load-bearing intracellular transport demands.

Future structural, biochemical, and motility assays are required to determine the mechanisms by which multiple dynein motors bound to the same dynactin–cargo adaptor complexes coordinate motor domain activity during processive transport of cellular cargo. As a dynamic motor, there are many other states within the mechanochemical cycle that will need to be investigated further to fully understand how these co-factors promote processive motility and to determine the precise "stepping patterns" of the individual motors within these massive assemblies. Additionally, the mechanisms and allostery through which cytoplasmic dynein and kinesin communicate to influence activity during bidirectional transport still remain unknown. It is possible that the conformational changes observed in IFT dynein are also utilized as a regulatory mechanism by cytoplasmic dynein, although further structural studies are needed to confirm such a mechanistic conservation. Finally, cytoplasmic dynein complexes have yet to be observed *in situ*, and future structural studies will likely depend on the development of sophisticated labeling and image-processing techniques to identify cytoplasmic dynein within the crowded cellular environment.

Emerging commonalities among dynein motors

Despite their conserved dynein heavy chain structure and mechanochemical cycle (24, 25), the three main groups of dynein motors (axonemal, IFT, and intracellular cytoplasmic dynein) tend to be investigated and considered as distinct entities within the dynein motor field. However, as additional structures of these dynamic transport systems are solved in the context of their native or near-native transport environment by tomography and subtomogram averaging (65, 83, 93, 130), structural and mechanistic commonalities are beginning to emerge (Fig. 6). Collectively, these studies suggest that all dynein motors may be equipped with fundamental core properties upon which evolution has layered context-specific regulation to endow dyneins with specialized functions. Whereas robust experimentation will be required to determine whether specific regulatory modalities are conserved across all members of the dynein superfamily, we propose that a recognition of the fundamental similarities shared by dynein motors will guide and facilitate the development of testable experimental models and predictions for dynein motor regulation and function, thereby benefitting and advancing the collective dynein motor field. Below, we outline the four unifying mechanisms of regulation that we see emerging within the dynein motor field.

Anchoring of tail domain to promote a propensity for forward, minus-end directed motility

It was previously hypothesized that the dynein motor subtypes may operate under a consistent mechanism across different systems in the cell (axonemal, IFT, and cytoplasmic), but in the absence of structural evidence, it remained speculative (7). Comparing recent structures solved by subtomogram averaging of "active" axonemal and cytoplasmic dynein reveals striking similarities, including the overall spatial organization of the motor domains bound to the microtubule, as well as the overall morphology of the tail domain (19, 130). In both structures, the motor domains are oriented parallel to one another, directed toward the minus-end of the microtubule. The dynein tail domains, which are composed of a series of helical bundles, extend from the motor domains and extensively interact with one another before associating with an elongated filamentous structure. In the case of axonemal dynein, this filamentous structure is a microtubule doublet, whereas the actin-like Arp1 filament of dynactin serves this role in the case of cytoplasmic dynein. Although a detailed structure of retrograde IFT trains with active IFT dynein molecules has yet to be elucidated, slices through a 3D tomogram of these trains reveals the presence of broad, zig-zagging structures that appear to anchor multiple IFT dyneins, suggesting that tethering of the IFT dynein tail influences the orientation of the motor domains to adopt a configuration that may resemble axonemal and cytoplasmic dynein (93).

This conserved organization of axonemal and cytoplasmic dyneins appears to stabilize the otherwise flexible tail and motor domains of dynein, and it may be an essential configuration that promotes efficient microtubule-based movement of all dynein motors. The conformational similarities observed in diverse cellular contexts suggest that cytoplasmic and IFT

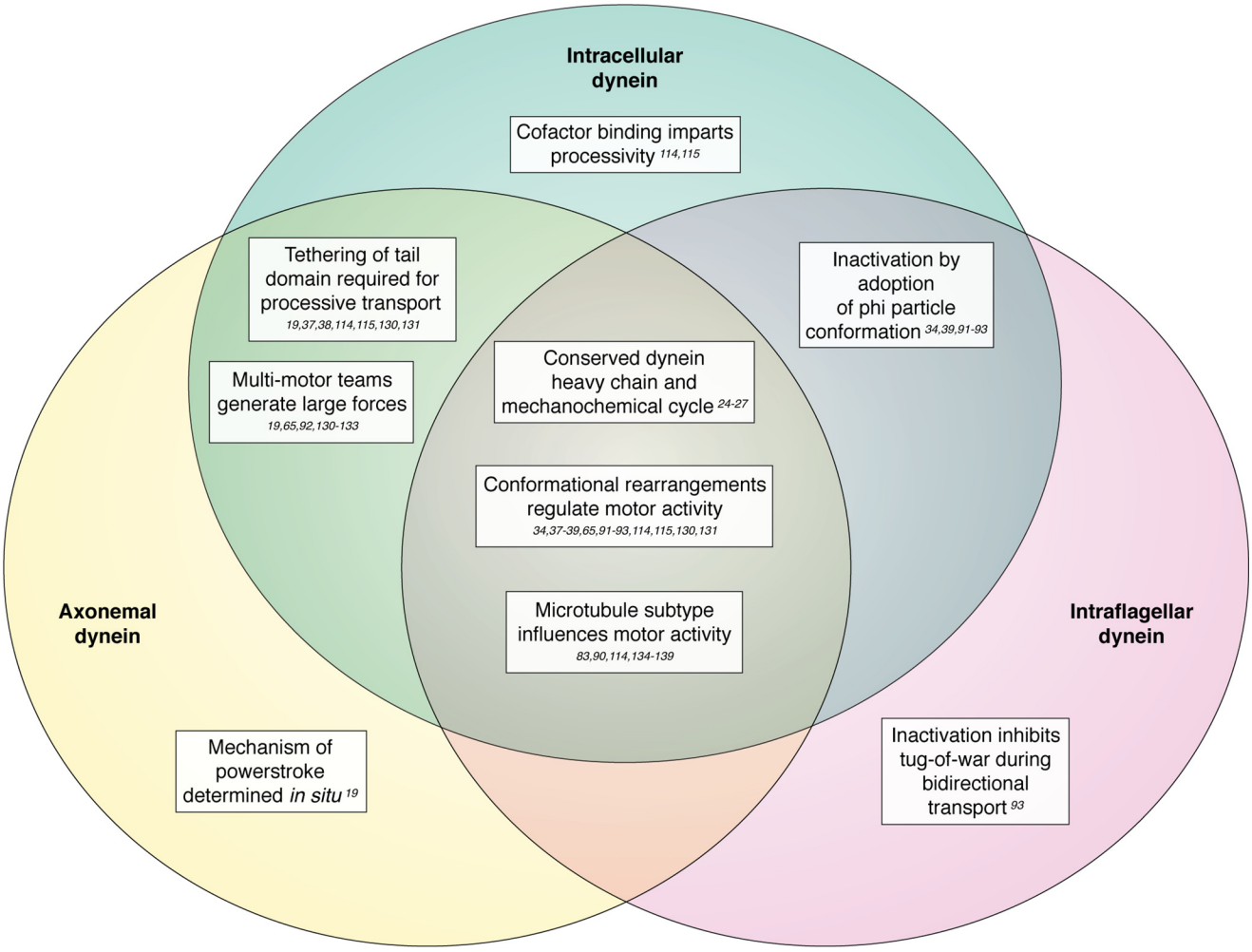

Figure 6. Emerging commonalities among members of the dynein motor superfamily. Observed functional and regulatory similarities among dynein motors are represented by *regions of overlap between colored circles*. We propose all stated functions are shared, but current technological hurdles limit our current understanding of different facets of dynein regulation. We speculate that technology development will give rise to structural and biochemical studies that will confirm these unifying mechanisms for all members of the dynein superfamily.

dynein utilize a mechanism that is similar to that used by axonemal dynein for minus-end directed motion (19). By associating the flexible tail domain of dynein with a scaffold—such as the A-tubule of the microtubule doublet for axonemal dynein, dynactin for cytoplasmic dynein, or the putative zig-zag structure of retrograde trains for IFT dynein—all dynein members confer an arrangement that orients the motor domains in a parallel position relative to the microtubule while accommodating the large-scale conformational changes associated with ATP hydrolysis in the motor domain ring that propel the microtubule-binding domain more effectively toward the microtubule minus-end. This model has been demonstrated *in situ* by tomography and subtomogram averaging to be the structural mechanism by which axonemal motors translocate along microtubules to accomplish flagellar motility, and it has also been proposed by several groups to be the mechanism utilized by cytoplasmic dynein (7, 19). Confirmation of this mechanism for cytoplasmic and IFT dynein will require the development of methods that capture snapshots of these motors in complex with their respective scaffold anchors while actively translocating along microtubules. Cryo-electron tomography offers a promising method to directly test these mechanisms, although this will likely depend on the development of more advanced subtomogram averaging and 3D classification approaches to distinguish between all of structural states of dynein motors in action.

Teamwork among multimotor assemblies

The direct observation that all members of the dynein protein family organize into multimotor assemblies suggests that collective movement as a "team" of motors may be an underlying mechanistic principle upon which additional structural features have evolved to carry out their diverse cellular functions. Thousands of axonemal dyneins arranged along the length and circumference of axonemal microtubules work together in a highly coordinated, regulated fashion to power flagellar motility, and cytoplasmic dynein can be recruited as pairs of dimers to a single dynactin– cargo adaptor scaffold to produce a more effective motor (130, 131). Both of these observations demonstrate a propensity for teamwork among multiple motors to drive intracellular transport of cytoplasmic cargo. Although a detailed structure of activated IFT dynein has not yet emerged from experimental data, 3D tomograms strongly suggest that multiple IFT dynein motors organize onto a single structure

scaffold (93), and therefore they are also likely to work collectively as part of IFT transport mechanism. In agreement with these results, previous work using a constructed DNA chassis to reconstitute an IFT train system showed that multimotor assemblies (~7 IFT dyneins) exhibit robust, processive minus-end motility, suggesting that teams of activated IFT dynein motors are also required for robust retrograde movement of IFT trains (92). Collectively, these results suggest that grouping multiple dynein motors together converts relatively weak individual dynein motors into large, fine-tunable, force-producing engines for cellular function (132, 133). Further investigation will be required to assess whether there are direct or indirect longitudinal interactions between dynein motors, and whether these interactions are directly mediated through structural rearrangements of dynein subunits and/or dependent on chemical modifications introduced by dynein regulatory proteins to coordinate this teamwork functionality.

Microtubule subtype influences motor activity

The microtubule tracks utilized by dynein motors can be heavily decorated with a myriad of post-translational modifications of α- and β-tubulin subunits, including tyrosination, acetylation, and glutamylation, which results in a diverse array of microtubule subtypes. These modifications can augment the structural integrity of microtubules (reviewed in Ref. (88), and numerous studies indicate that this microtubule diversity contributes to the differential regulation of dynein motor activity and subcellular localization. The microtubule C-terminal tails are the target of the vast majority of modifications, and *in vitro* reconstituted motility assays show that tail deletion reduces processivity of purified yeast cytoplasmic dynein, cytoplasmic dynein-coated beads, and mammalian DDB complexes along microtubules (90, 114, 134). Additionally, several studies specifically implicate C-terminal tail tyrosination as essential for mammalian cytoplasmic dynein motility, likely mediated through dynactin's p150Glued subunit CAP–Gly domain, because *in situ* studies show that both DDB complexes and dynein-driven neuronal cargo selectively initiate transport on tyrosinated microtubules, rather than detyrosinated microtubules (135, 136). In contrast, the activity of axonemal dyneins appears to be regulated by C-terminal tail glutamylation, as the lack of polyglutamate chains on α-tubulin affects the function of axonemal inner-arm dyneins (137, 138). Interestingly, the acetylation of a single lysine residue on tubulin, located within the inner luminal surface of the microtubule, is required for efficient motility of *Chlamydomonas* axonemal outer-arm dyneins (139). It is unclear how a luminal microtubule modification could affect the activity of dynein motors translocating on the outer microtubule surface, and further investigation is needed to determine whether axonemal dyneins sense this modification through direct or indirect mechanisms. Recent CLEM studies from Sepanek and Pigino (83) demonstrate that the microtubule subtype may play a regulatory role in the specificity of IFT dynein motors for A-tubules over B-tubules. However, further studies are required to elucidate the precise molecular mechanisms responsible for this specificity and whether post-translational modifications on tubulin subunits play a direct role in IFT dynein motility. Regardless of the exact nature of these modifications, these studies collectively demonstrate that all members of the dynein motor superfamily can sense, either through direct or perhaps indirect mechanisms, diversity in cellular microtubule subtypes, which in turn profoundly affects motility and cellular function.

Conformational rearrangements to regulate dynein activity

Recent structural studies have revealed that all dynein motors can adopt distinct, structurally recognizable "active" and "inactive" conformations, suggesting that all motors are regulated by long-range structural rearrangements of dynein, which subsequently influences activity. For example, both IFT and cytoplasmic dyneins adopt the "ϕ-particle" conformation, wherein stacking of the AAA+ rings renders dynein motors incapable of microtubule binding and ATP hydrolysis (34, 39, 91–93). Specific molecular interactions between cytoplasmic dynein motors and cofactors are necessary to relieve this auto-inhibition and reorient the motor domains in an active conformation amenable for microtubule-based transport (Fig. 5) (37, 130). Because of the similarities observed in these two disparate systems, it is tempting to speculate that anterograde-directed transport that does not exhibit tug–of–war behavior requires cytoplasmic dynein to adopt an inactive ϕ conformation similar to that of IFT dynein. However, future structural and functional assays are required to test this possibility.

Whereas the ϕ-particle conformation has not yet been observed for axonemal dyneins, it is possible that axonemal dyneins may adopt the "ϕ-particle" conformation within the cytoplasm, prior to assembly of the axoneme structure (65, 146). However, further structural, biochemical, and cellular studies are required to test this hypothesis directly. Importantly, it is evident from a myriad of previous structures solved by subtomogram averaging that the activity of axonemal dyneins can be defined by the orientation of the dynein tail, AAA+ ring, stalk, and microtubule-binding domain relative to the corresponding B-tubule such that a small angle between the tail and stalk domain represents an "inactive" conformation, whereas a large angle between these structures represents an "active" conformation in which dynein is actively progressing through the force-producing mechanochemical cycle (27, 65). It will be interesting to test whether these conformations are functionally relevant to IFT and cytoplasmic dyneins during microtubule-based transport. Further structural, biochemical, and motility assay experiments are necessary to ultimately test whether these facets of dynein activity regulation can be applied to all members of the dynein motor superfamily.

Cellular electron tomography: the future of dynein structure determination

During the 5 decades since Gibbon and Grimstone's initial discovery of dynein microtubule motor (28), the field has advanced significantly toward understanding the structure, function, and regulation of all members of the dynein motor protein family. Recent methodological improvements in the field of electron tomography have enabled researchers to visualize snapshots of dynamic dynein motor proteins within their respective transport environments, providing a structural con-

text for decades of biophysical and biochemical research on dynein regulation and function. However, much like a Russian nesting doll, as new mechanistic insights are unveiled, additional uncharted layers of fascinating complexity emerge, presenting further questions about the function and regulation of these diverse, force-producing engines.

Looking ahead, cryo-electron tomography holds the potential to become the principal high-resolution imaging technique in cell biology, and it is likely to fundamentally change the way in which researchers in the dynein motor protein field (and likely many biological fields) investigate these challenging, outstanding questions (Fig. 2*E*). For example, a technique called cryo-focused ion beam milling uses a focused beam of ions to remove large sections of frozen cells without devitrifying the sample to generate a single thin layer (lamella) of cellular material. This technique makes it possible to expose the organelles and macromolecular systems that are buried within regions of the eukaryotic cells that are too thick to image by traditional transmission EM (140). Imaged in the electron microscope, these lamellae are reminiscent of the microtomed sections of cells that led to the initial discovery of dynein (Fig. 2*A*), but are free of the dehydration and staining artifacts introduced by epoxy-embedding methodologies (141). By combining cryo-electron tomography data collection schemes with phase plate technology, which dramatically increases the phase contrast within EM images, researchers can image these thin lamellae to produce unprecedented views of the subcellular organization of thousands of macromolecules pristinely preserved with minimal perturbation to their native *in situ* structure (142–145). Furthermore, technological improvements to CLEM approaches offer the exciting promise of improving both the spatial and temporal correlation between complementary imaging modalities (reviewed in Ref. 123), setting the stage to combine dynamic, real-time, and live-cell fluorescence imaging with cryo-preserved, high-resolution cryo-electron tomography analyses. Given the inherent, dynamic functionality of motile dynein complexes, these combined cellular tomography approaches will likely dramatically improve our understanding of dynein motors, both in the context of cellular homeostasis and in dynein-associated disease pathology.

References

1. Eschbach, J., and Dupuis, L. (2011) Cytoplasmic dynein in neurodegeneration. *Pharmacol. Ther.* **130,** 348–363 CrossRef Medline
2. Kempeneers, C., and Chilvers, M. A. (2018) To beat, or not to beat, that is question! The spectrum of ciliopathies. *Pediatr. Pulmonol.* **53,** 1122–1129 CrossRef Medline
3. Reiter, J. F., and Leroux, M. R. (2017) Genes and molecular pathways underpinning ciliopathies. *Nat. Rev. Mol. Cell Biol.* **18,** 533–547 CrossRef Medline
4. Gee, M. A., Heuser, J. E., and Vallee, R. B. (1997) An extended microtubule-binding structure within the dynein motor domain. *Nature* **390,** 636–639 CrossRef Medline
5. Samsó, M., Radermacher, M., Frank, J., and Koonce, M. P. (1998) Structural characterization of a dynein motor domain. *J. Mol. Biol.* **276,** 927–937 CrossRef Medline
6. Koonce, M. P., and Tikhonenko, I. (2000) Functional elements within the dynein microtubule-binding domain. *Mol. Biol. Cell.* **11,** 523–529 CrossRef Medline
7. Burgess, S. A., Walker, M. L., Sakakibara, H., Knight, P. J., and Oiwa, K. (2003) Dynein structure and power stroke. *Nature* **421,** 715–718 CrossRef Medline
8. Samsó, M., and Koonce, M. P. (2004) 25 Å resolution structure of a cytoplasmic dynein motor reveals a seven-member planar ring. *J. Mol. Biol.* **340,** 1059–1072 CrossRef Medline
9. Gibbons, I. R., Garbarino, J. E., Tan, C. E., Reck-Peterson, S. L., Vale, R. D., and Carter, A. P. (2005) The affinity of the dynein microtubule-binding domain is modulated by the conformation of its coiled-coil stalk. *J. Biol. Chem.* **280,** 23960–23965 CrossRef Medline
10. Mizuno, N., Narita, A., Kon, T., Sutoh, K., and Kikkawa, M. (2007) Three-dimensional structure of cytoplasmic dynein bound to microtubules. *Proc. Natl. Acad. Sci. U.S.A.* **104,** 20832–20837 CrossRef Medline
11. Carter, A. P., Garbarino, J. E., Wilson-Kubalek, E. M., Shipley, W. E., Cho, C., Milligan, R. A., Vale, R. D., and Gibbons, I. R. (2008) Structure and functional role of dynein's microtubule-binding domain. *Science* **322,** 1691–1695 CrossRef Medline
12. Carter, A. P., Cho, C., Jin, L., and Vale, R. D. (2011) Crystal structure of the dynein motor domain. *Science* **331,** 1159–1165 CrossRef Medline
13. Kon, T., Sutoh, K., and Kurisu, G. (2011) X-ray structure of a functional full-length dynein motor domain. *Nat. Struct. Mol. Biol.* **18,** 638–642 CrossRef Medline
14. Roberts, A. J., Numata, N., Walker, M. L., Kato, Y. S., Malkova, B., Kon, T., Ohkura, R., Arisaka, F., Knight, P. J., Sutoh, K., and Burgess, S. A. (2009) AAA+ ring and linker swing mechanism in the dynein motor. *Cell* **136,** 485–495 CrossRef Medline
15. Roberts, A. J., Malkova, B., Walker, M. L., Sakakibara, H., Numata, N., Kon, T., Ohkura, R., Edwards, T. A., Knight, P. J., Sutoh, K., Oiwa, K., and Burgess, S. A. (2012) ATP-driven remodeling of the linker domain in the dynein motor. *Structure* **20,** 1670–1680 CrossRef Medline
16. Schmidt, H., Gleave, E. S., and Carter, A. P. (2012) Insights into dynein motor domain function from a 3.3-Å crystal structure. *Nat. Struct. Mol. Biol.* **19,** 492–497 CrossRef Medline
17. Redwine, W. B., Hernandez-López, R., Zou, S., Huang, J., Reck-Peterson, S. L., and Leschziner, A. E. (2012) Structural basis for microtubule binding and release by dynein. *Science* **337,** 1532–1536 CrossRef Medline
18. Bhabha, G., Cheng, H.-C., Zhang, N., Moeller, A., Liao, M., Speir, J. A., Cheng, Y., and Vale, R. D. (2014) Allosteric communication in the dynein motor domain. *Cell* **159,** 857–868 CrossRef Medline
19. Lin, J., Okada, K., Raytchev, M., Smith, M. C., and Nicastro, D. (2014) Structural mechanism of the dynein powerstroke. *Nat. Cell Biol.* **16,** 479–485 CrossRef Medline
20. Schmidt, H., Zalyte, R., Urnavicius, L., and Carter, A. P. (2015) Structure of human cytoplasmic dynein-2 primed for its power stroke. *Nature* **518,** 435–438 CrossRef Medline
21. Habura, A., Tikhonenko, I., Chisholm, R. L., and Koonce, M. P. (1999) Interaction mapping of a dynein heavy chain. Identification of dimerization and intermediate-chain binding domains. *J. Biol. Chem.* **274,** 15447–15453 CrossRef Medline
22. Tynan, S. H., Gee, M. A., and Vallee, R. B. (2000) Distinct but overlapping sites within the cytoplasmic dynein heavy chain for dimerization and for intermediate chain and light intermediate chain binding. *J. Biol. Chem.* **275,** 32769–32774 CrossRef Medline
23. Qiu, R., Zhang, J., and Xiang, X. (2013) Identification of a novel site in the tail of dynein heavy chain important for dynein function *in vivo*. *J. Biol. Chem.* **288,** 2271–2280 CrossRef Medline
24. Cho, C., and Vale, R. D. (2012) The mechanism of dynein motility: insight from crystal structures of the motor domain. *Biochim. Biophys. Acta* **1823,** 182–191 CrossRef Medline
25. Carter, A. P. (2013) Crystal clear insights into how the dynein motor moves. *J. Cell Sci.* **126,** 705–713 CrossRef Medline
26. Cianfrocco, M. A., DeSantis, M. E., Leschziner, A. E., and Reck-Peterson, S. L. (2015) Mechanism and regulation of cytoplasmic dynein. *Annu. Rev. Cell Dev. Biol.* **31,** 83–108 CrossRef Medline
27. Schmidt, H., and Carter, A. P. (2016) Review: structure and mechanism of the dynein motor ATPase. *Biopolymers* **105,** 557–567 CrossRef Medline

28. Gibbons, I. R., and Grimstone, A. V. (1960) On flagellar structure in certain flagellates. *J. Biophys. Biochem. Cytol.* **7,** 697–716 CrossRef Medline
29. Warner, F. D., and Mitchell, D. R. (1978) Structural conformation of ciliary dynein arms and the generation of sliding forces in *Tetrahymena* cilia. *J. Cell Biol.* **76,** 261–277 CrossRef Medline
30. Goodenough, U. W., and Heuser, J. E. (1982) Substructure of the outer dynein arm. *J. Cell Biol.* **95,** 798–815 CrossRef Medline
31. Goodenough, U., and Heuser, J. (1984) Structural comparison of purified dynein proteins with *in situ* dynein arms. *J. Mol. Biol.* **180,** 1083–1118 CrossRef Medline
32. Sale, W. S., Goodenough, U. W., and Heuser, J. E. (1985) The substructure of isolated and *in situ* outer dynein arms of sea urchin sperm flagella. *J. Cell Biol.* **101,** 1400–1412 CrossRef Medline
33. Vallee, R. B., Wall, J. S., Paschal, B. M., and Shpetner, H. S. (1988) Microtubule-associated protein 1C from brain is a two-headed cytosolic dynein. *Nature* **332,** 561–563 CrossRef Medline
34. Amos, L. A. (1989) Brain dynein crossbridges microtubules into bundles. *J. Cell Sci.* **93,** 19–28 Medline
35. Takahashi, M., and Tonomura, Y. (1978) Binding of 30s dynein with the B-tubule of the outer doublet of axonemes from *Tetrahymena pyriformis* and adenosine triphosphate-induced dissociation of the complex. *J. Biochem.* **84,** 1339–1355 CrossRef Medline
36. Pazour, G. J., Wilkerson, C. G., and Witman, G. B. (1998) A dynein light chain is essential for the retrograde particle movement of intraflagellar transport (IFT). *J. Cell Biol.* **141,** 979–992 CrossRef Medline
37. Chowdhury, S., Ketcham, S. A., Schroer, T. A., and Lander, G. C. (2015) Structural organization of the dynein–dynactin complex bound to microtubules. *Nat. Struct. Mol. Biol.* **22,** 345–347 CrossRef Medline
38. Urnavicius, L., Zhang, K., Diamant, A. G., Motz, C., Schlager, M. A., Yu, M., Patel, N. A., Robinson, C. V., and Carter, A. P. (2015) The structure of the dynactin complex and its interaction with dynein. *Science* **347,** 1441–1446 CrossRef Medline
39. Zhang, K., Foster, H. E., Rondelet, A., Lacey, S. E., Bahi-Buisson, N., Bird, A. W., and Carter, A. P. (2017) Cryo-EM reveals how human cytoplasmic dynein is auto-inhibited and activated. *Cell* **169,** 1303–1314.e18 CrossRef Medline
40. Lučić, V., Rigort, A., and Baumeister, W. (2013). Cryo-electron tomography: The challenge of doing structural biology in situ. *J Cell Biol.* **202,** 407–419 CrossRef Medline
41. Oikonomou, C. M., and Jensen, G. J. (2017) Cellular electron cryotomography: toward structural biology *in situ*. *Annu. Rev. Biochem.* **86,** 873–896 CrossRef Medline
42. Himes, B. A., and Zhang, P. (2018) emClarity: software for high-resolution cryo-electron tomography and subtomogram averaging. *Nat. Methods* **15,** 955–961 CrossRef Medline
43. Briggs, J. A. (2013) Structural biology *in situ*—the potential of subtomogram averaging. *Curr. Opin Struct. Biol.* **23,** 261–267 CrossRef Medline
44. Nicastro, D., Schwartz, C., Pierson, J., Gaudette, R., Porter, M. E., and McIntosh, J. R. (2006) The molecular architecture of axonemes revealed by cryoelectron tomography. *Science* **313,** 944–948 CrossRef Medline
45. Movassagh, T., Bui, K. H., Sakakibara, H., Oiwa, K., and Ishikawa, T. (2010) Nucleotide-induced global conformational changes of flagellar dynein arms revealed by *in situ* analysis. *Nat. Struct. Mol. Biol.* **17,** 761–767 CrossRef Medline
46. Heuser, T., Barber, C. F., Lin, J., Krell, J., Rebesco, M., Porter, M. E., and Nicastro, D. (2012) Cryoelectron tomography reveals doublet-specific structures and unique interactions in the I1 dynein. *Proc. Natl. Acad. Sci. U.S.A.* **109,** E2067–E2076 CrossRef Medline
47. Oda, T., Yanagisawa, H., and Kikkawa, M. (2015) Detailed structural and biochemical characterization of the nexin–dynein regulatory complex. *Mol. Biol. Cell.* **26,** 294–304 CrossRef Medline
48. Nicastro, D. (2009) Cryo-electron microscope tomography to study axonemal organization. *Methods Cell Biol.* **91,** 1–39 CrossRef Medline
49. Ishikawa, T. (2015) Cryo-electron tomography of motile cilia and flagella. *Cilia 2015* **4,** 3 CrossRef Medline
50. Gibbons, I. R., and Rowe, A. J. (1965) Dynein: a protein with adenosine triphosphatase activity from cilia. *Science* **149,** 424–426 CrossRef Medline
51. Mitchell, D. R., and Rosenbaum, J. L. (1985) A motile *Chlamydomonas* flagellar mutant that lacks outer dynein arms. *J. Cell Biol.* **100,** 1228–1234 CrossRef Medline
52. Okagaki, T., and Kamiya, R. (1986) Microtubule sliding in mutant *Chlamydomonas* axonemes devoid of outer or inner dynein arms. *J. Cell Biol.* **103,** 1895–1902 CrossRef Medline
53. Vale, R. D., and Toyoshima, Y. Y. (1989) Microtubule translocation properties of intact and proteolytically digested dyneins from *Tetrahymena* cilia. *J. Cell Biol.* **108,** 2327–2334 CrossRef Medline
54. Kamiya, R., and Yagi, T. (2014) Functional diversity of axonemal dyneins as assessed by *in vitro* and *in vivo* motility assays of *Chlamydomonas* mutants. *Zoolog. Sci.* **31,** 633–644 CrossRef Medline
55. Gokhale, A., Wirschell, M., and Sale, W. S. (2009) Regulation of dynein-driven microtubule sliding by the axonemal protein kinase CK1 in *Chlamydomonas* flagella. *J. Cell Biol.* **186,** 817–824 CrossRef Medline
56. Hayashi, S., and Shingyoji, C. (2008) Mechanism of flagellar oscillation-bending-induced switching of dynein activity in elastase-treated axonemes of sea urchin sperm. *J. Cell Sci.* **121,** 2833–2843 CrossRef Medline
57. Mitchison, T. J., and Mitchison, H. M. (2010) How cilia beat. *Nature* **463,** 308–309 CrossRef Medline
58. Mizuno, N., Taschner, M., Engel, B. D., and Lorentzen, E. (2012) Structural studies of ciliary components. *J. Mol. Biol.* **422,** 163–180 CrossRef Medline
59. Sale, W. S. (1986) The axonemal axis and Ca^{2+}-induced asymmetry of active microtubule sliding in sea urchin sperm tails. *J. Cell Biol.* **102,** 2042–2052 CrossRef Medline
60. Sale, W. S., and Satir, P. (1977) Direction of active sliding of microtubules in *Tetrahymena* cilia. *Proc. Natl. Acad. Sci. U.S.A.* **74,** 2045–2049 CrossRef Medline
61. Smith, E. F., and Sale, W. S. (1992) Regulation of dynein-driven microtubule sliding by the radial spokes in flagella. *Science* **257,** 1557–1559 CrossRef Medline
62. Summers, K. E., and Gibbons, I. R. (1971) Adenosine triphosphate-induced sliding of tubules in trypsin-treated flagella of sea-urchin sperm. *Proc. Natl. Acad. Sci. U.S.A.* **68,** 3092–3096 CrossRef Medline
63. Tamm, S. L., and Tamm, S. (1984) Alternate patterns of doublet microtubule sliding in ATP-disintegrated macrocilia of the ctenophore *Beroe*. *J. Cell Biol.* **99,** 1364–1371 CrossRef Medline
64. Wais-Steider, J., and Satir, P. (1979) Effect of vanadate on gill cilia: switching mechanism in ciliary beat. *J. Supramol. Struct.* **11,** 339–347 CrossRef Medline
65. Lin, J., and Nicastro, D. (2018) Asymmetric distribution and spatial switching of dynein activity generates ciliary motility. *Science* **360,** eaar1968 CrossRef Medline
66. Ringo, D. L. (1967) Flagellar motion and fine structure of the flagellar apparatus in *Chlamydomonas*. *J. Cell Biol.* **33,** 543–571 CrossRef Medline
67. Kozminski, K. G., Johnson, K. A., Forscher, P., and Rosenbaum, J. L. (1993) A motility in the eukaryotic flagellum unrelated to flagellar beating. *Proc. Natl. Acad. Sci. U.S.A.* **90,** 5519–5523 CrossRef Medline
68. Kozminski, K. G., Beech, P. L., and Rosenbaum, J. L. (1995) The *Chlamydomonas* kinesin-like protein FLA10 is involved in motility associated with the flagellar membrane. *J. Cell Biol.* **131,** 1517–1527 CrossRef Medline
69. Cole, D. G., Diener, D. R., Himelblau, A. L., Beech, P. L., Fuster, J. C., and Rosenbaum, J. L. (1998) *Chlamydomonas* kinesin-II-dependent intraflagellar transport (IFT): IFT particles contain proteins required for ciliary assembly in *Caenorhabditis elegans* sensory neurons. *J. Cell Biol.* **141,** 993–1008 CrossRef Medline
70. Porter, M. E., Bower, R., Knott, J. A., Byrd, P., and Dentler, W. (1999) Cytoplasmic dynein heavy chain 1b is required for flagellar assembly in *Chlamydomonas*. *Mol. Biol. Cell.* **10,** 693–712 CrossRef Medline
71. Hou, Y., Pazour, G. J., and Witman, G. B. (2004) A dynein light intermediate chain, D1bLIC, is required for retrograde intraflagellar transport. *Mol. Biol. Cell.* **15,** 4382–4394 CrossRef Medline
72. Pigino, G., Geimer, S., Lanzavecchia, S., Paccagnini, E., Cantele, F., Diener, D. R., Rosenbaum, J. L., and Lupetti, P. (2009) Electron-tomographic analysis of intraflagellar transport particle trains *in situ*. *J. Cell Biol.* **187,** 135–148 CrossRef Medline

73. Vale, R. D., and Milligan, R. A. (2000) The way things move: looking under the hood of molecular motor proteins. *Science* **288,** 88–95 CrossRef Medline
74. Yildiz, A., Tomishige, M., Vale, R. D., and Selvin, P. R. (2004) Kinesin walks hand-over-hand. *Science* **303,** 676–678 CrossRef Medline
75. Qiu, W., Derr, N. D., Goodman, B. S., Villa, E., Wu, D., Shih, W., and Reck-Peterson, S. L. (2012) Dynein achieves processive motion using both stochastic and coordinated stepping. *Nat. Struct. Mol. Biol.* **19,** 193–200 CrossRef Medline
76. Piperno, G., and Mead, K. (1997) Transport of a novel complex in the cytoplasmic matrix of *Chlamydomonas* flagella. *Proc. Natl. Acad. Sci. U.S.A.* **94,** 4457–4462 CrossRef Medline
77. Qin, H., Diener, D. R., Geimer, S., Cole, D. G., and Rosenbaum, J. L. (2004) Intraflagellar transport (IFT) cargo. *J. Cell Biol.* **164,** 255–266 CrossRef Medline
78. Vannuccini, E., Paccagnini, E., Cantele, F., Gentile, M., Dini, D., Fino, F., Diener, D., Mencarelli, C., and Lupetti, P. (2016) Two classes of short intraflagellar transport train with different 3D structures are present in *Chlamydomonas* flagella. *J. Cell Sci.* **129,** 2064–2074 CrossRef Medline
79. Reck, J., Schauer, A. M., VanderWaal Mills, K., Bower, R., Tritschler, D., Perrone, C. A., and Porter, M. E. (2016) The role of the dynein light intermediate chain in retrograde IFT and flagellar function in *Chlamydomonas*. *Mol. Biol. Cell.* **27,** 2404–2422 CrossRef Medline
80. Buisson, J., Chenouard, N., Lagache, T., Blisnick, T., Olivo-Marin, J.-C., and Bastin, P. (2013) Intraflagellar transport proteins cycle between the flagellum and its base. *J. Cell Sci.* **126,** 327–338 CrossRef Medline
81. Wren, K. N., Craft, J. M., Tritschler, D., Schauer, A., Patel, D. K., Smith, E. F., Porter, M. E., Kner, P., and Lechtreck, K. F. (2013) A differential cargo-loading model of ciliary length regulation by IFT. *Curr. Biol.* **23,** 2463–2471 CrossRef Medline
82. Chien, A., Shih, S. M., Bower, R., Tritschler, D., Porter, M. E., and Yildiz, A. (2017) Dynamics of the IFT machinery at the ciliary tip. *Elife* **6,** e28606 CrossRef Medline
83. Stepanek, L., and Pigino, G. (2016) Microtubule doublets are double-track railways for intraflagellar transport trains. *Science* **352,** 721–724 CrossRef Medline
84. Stepanek, L., and Pigino, G. (2017) Millisecond time resolution correlative light and electron microscopy for dynamic cellular processes. *Methods Cell Biol.* **140,** 1–20 CrossRef Medline
85. Rogowski, M., Scholz, D., and Geimer, S. (2013) Electron microscopy of flagella, primary cilia, and intraflagellar transport in flat-embedded cells. *Methods Enzymol.* **524,** 243–263 CrossRef Medline
86. Johnson, K. A. (1998) The axonemal microtubules of the *Chlamydomonas* flagellum differ in tubulin isoform content. *J. Cell Sci.* **111,** 313–320 Medline
87. Garnham, C. P., and Roll-Mecak, A. (2012) The chemical complexity of cellular microtubules: tubulin post-translational modification enzymes and their roles in tuning microtubule functions. *Cytoskeleton* **69,** 442–463 CrossRef Medline
88. Yu, I., Garnham, C. P., and Roll-Mecak, A. (2015) Writing and reading the tubulin code. *J. Biol. Chem.* **290,** 17163–17172 CrossRef Medline
89. Konishi, Y., and Setou, M. (2009) Tubulin tyrosination navigates the kinesin-1 motor domain to axons. *Nat. Neurosci.* **12,** 559–567 CrossRef Medline
90. Sirajuddin, M., Rice, L. M., and Vale, R. D. (2014) Regulation of microtubule motors by tubulin isotypes and post-translational modifications. *Nat. Cell Biol.* **16,** 335–344 CrossRef Medline
91. Torisawa, T., Ichikawa, M., Furuta, A., Saito, K., Oiwa, K., Kojima, H., Toyoshima, Y. Y., and Furuta, K. (2014) Autoinhibition and cooperative activation mechanisms of cytoplasmic dynein. *Nat. Cell Biol.* **16,** 1118–1124 CrossRef Medline
92. Toropova, K., Mladenov, M., and Roberts, A. J. (2017) Intraflagellar transport dynein is autoinhibited by trapping of its mechanical and track-binding elements. *Nat. Struct. Mol. Biol.* **24,** 461–468 CrossRef Medline
93. Jordan, M. A., Diener, D. R., Stepanek, L., and Pigino, G. (2018) The cryo-EM structure of intraflagellar transport trains reveals how dynein is inactivated to ensure unidirectional anterograde movement in cilia. *Nat. Cell Biol.* **20,** 1250–1255 CrossRef Medline
94. Hollenbeck, P. J., and Saxton, W. M. (2005) The axonal transport of mitochondria. *J. Cell Sci.* **118,** 5411–5419 CrossRef Medline
95. Pilling, A. D., Horiuchi, D., Lively, C. M., and Saxton, W. M. (2006) Kinesin-1 and dynein are the primary motors for fast transport of mitochondria in *Drosophila* motor axons. *Mol. Biol. Cell.* **17,** 2057–2068 CrossRef Medline
96. Driskell, O. J., Mironov, A., Allan, V. J., and Woodman, P. G. (2007) Dynein is required for receptor sorting and the morphogenesis of early endosomes. *Nat. Cell Biol.* **9,** 113–120 CrossRef Medline
97. Tan, S. C., Scherer, J., and Vallee, R. B. (2011) Recruitment of dynein to late endosomes and lysosomes through light intermediate chains. *Mol. Biol. Cell.* **22,** 467–477 CrossRef Medline
98. Jordens, I., Fernandez-Borja, M., Marsman, M., Dusseljee, S., Janssen, L., Calafat, J., Janssen, H., Wubbolts, R., and Neefjes, J. (2001) The Rab7 effector protein RILP controls lysosomal transport by inducing the recruitment of dynein–dynactin motors. *Curr. Biol.* **11,** 1680–1685 CrossRef Medline
99. Blocker, A., Severin, F. F., Burkhardt, J. K., Bingham, J. B., Yu, H., Olivo, J. C., Schroer, T. A., Hyman, A. A., and Griffiths, G. (1997) Molecular requirements for bi-directional movement of phagosomes along microtubules. *J. Cell Biol.* **137,** 113–129 CrossRef Medline
100. Gross, S. P., Tuma, M. C., Deacon, S. W., Serpinskaya, A. S., Reilein, A. R., and Gelfand, V. I. (2002) Interactions and regulation of molecular motors in *Xenopus* melanophores. *J. Cell Biol.* **156,** 855–865 CrossRef Medline
101. Vancoillie, G., Lambert, J., Mulder, A., Koerten, H. K., Mommaas, A. M., Van Oostveldt, P., and Naeyaert, J. M. (2000) Cytoplasmic dynein colocalizes with melanosomes in normal human melanocytes. *Br. J. Dermatol.* **143,** 298–306 CrossRef Medline
102. Kural, C., Kim, H., Syed, S., Goshima, G., Gelfand, V. I., and Selvin, P. R. (2005) Kinesin and dynein move a peroxisome *in vivo*: a tug-of-war or coordinated movement? *Science* **308,** 1469–1472 CrossRef Medline
103. Hsu, M.-T., Guo, C.-L., Liou, A. Y., Chang, T.-Y., Ng, M.-C., Florea, B. I., Overkleeft, H. S., Wu, Y.-L., Liao, J.-C., and Cheng, P.-L. (2015) Stage-dependent axon transport of proteasomes contributes to axon development. *Dev. Cell* **35,** 418–431 CrossRef Medline
104. Gross, S. P., Welte, M. A., Block, S. M., and Wieschaus, E. F. (2000) Dynein-mediated cargo transport *in vivo*. A switch controls travel distance. *J. Cell Biol.* **148,** 945–956 CrossRef Medline
105. Dodding, M. P., and Way, M. (2011) Coupling viruses to dynein and kinesin-1. *EMBO J.* **30,** 3527–3539 CrossRef Medline
106. Döhner, K., Wolfstein, A., Prank, U., Echeverri, C., Dujardin, D., Vallee, R., and Sodeik, B. (2002) Function of dynein and dynactin in herpes simplex virus capsid transport. *Mol. Biol. Cell.* **13,** 2795–2809 CrossRef Medline
107. Presley, J. F., Cole, N. B., Schroer, T. A., Hirschberg, K., Zaal, K. J., and Lippincott-Schwartz, J. (1997) ER-to-Golgi transport visualized in living cells. *Nature* **389,** 81–85 CrossRef Medline
108. Young, A., Dictenberg, J. B., Purohit, A., Tuft, R., and Doxsey, S. J. (2000) Cytoplasmic dynein-mediated assembly of pericentrin and gamma tubulin onto centrosomes. *Mol. Biol. Cell.* **11,** 2047–2056 CrossRef Medline
109. Harrell, J. M., Murphy, P. J., Morishima, Y., Chen, H., Mansfield, J. F., Galigniana, M. D., and Pratt, W. B. (2004) Evidence for glucocorticoid receptor transport on microtubules by dynein. *J. Biol. Chem.* **279,** 54647–54654 CrossRef Medline
110. Shah, J. V., Flanagan, L. A., Janmey, P. A., and Leterrier, J. F. (2000) Bidirectional translocation of neurofilaments along microtubules mediated in part by dynein/dynactin. *Mol. Biol. Cell.* **11,** 3495–3508 CrossRef Medline
111. Gagnon, J. A., and Mowry, K. L. (2011) Molecular motors: directing traffic during RNA localization. *Crit. Rev. Biochem. Mol. Biol.* **46,** 229–239 CrossRef Medline
112. Bader, J. R., Kasuboski, J. M., Winding, M., Vaughan, P. S., Hinchcliffe, E. H., and Vaughan, K. T. (2011) Polo-like kinase1 is required for recruitment of dynein to kinetochores during mitosis. *J. Biol. Chem.* **286,** 20769–20777 CrossRef Medline
113. Raaijmakers, J. A., and Medema, R. H. (2014) Function and regulation of dynein in mitotic chromosome segregation. *Chromosoma* **123,** 407–422 CrossRef Medline

114. McKenney, R. J., Huynh, W., Tanenbaum, M. E., Bhabha, G., and Vale, R. D. (2014) Activation of cytoplasmic dynein motility by dynactin–cargo adapter complexes. *Science* **345,** 337–341 CrossRef Medline
115. Schlager, M. A., Hoang, H. T., Urnavicius, L., Bullock, S. L., and Carter, A. P. (2014) *In vitro* reconstitution of a highly processive recombinant human dynein complex. *EMBO J.* **33,** 1855–1868 CrossRef Medline
116. Schroer, T. A., and Sheetz, M. P. (1991) Two activators of microtubule-based vesicle transport. *J. Cell Biol.* **115,** 1309–1318 CrossRef Medline
117. Gill, S. R., Schroer, T. A., Szilak, I., Steuer, E. R., Sheetz, M. P., and Cleveland, D. W. (1991) Dynactin, a conserved, ubiquitously expressed component of an activator of vesicle motility mediated by cytoplasmic dynein. *J. Cell Biol.* **115,** 1639–1650 CrossRef Medline
118. King, S. J., and Schroer, T. A. (2000) Dynactin increases the processivity of the cytoplasmic dynein motor. *Nat. Cell Biol.* **2,** 20–24 CrossRef Medline
119. Schroer, T. A. (2004) Dynactin. *Annu. Rev. Cell Dev. Biol.* **20,** 759–779 CrossRef Medline
120. Splinter, D., Razafsky, D. S., Schlager, M. A., Serra-Marques, A., Grigoriev, I., Demmers, J., Keijzer, N., Jiang, K., Poser, I., Hyman, A. A., Hoogenraad, C. C., King, S. J., and Akhmanova, A. (2012) BICD2, dynactin, and LIS1 cooperate in regulating dynein recruitment to cellular structures. *Mol. Biol. Cell.* **23,** 4226–4241 CrossRef Medline
121. Moore, J. K., Li, J., and Cooper, J. A. (2008) Dynactin function in mitotic spindle positioning. *Traffic* **9,** 510–527 CrossRef Medline
122. Moore, J. K., Sept, D., and Cooper, J. A. (2009) Neurodegeneration mutations in dynactin impair dynein-dependent nuclear migration. *Proc. Natl. Acad. Sci. U.S.A.* **106,** 5147–5152 CrossRef Medline
123. de Boer, P., Hoogenboom, J. P., and Giepmans, B. N. (2015) Correlated light and electron microscopy: ultrastructure lights up! *Nat. Methods.* **12,** 503–513 CrossRef Medline
124. Hoogenraad, C. C., Wulf, P., Schiefermeier, N., Stepanova, T., Galjart, N., Small, J. V., Grosveld, F., de Zeeuw, C. I., and Akhmanova, A. (2003) Bicaudal D induces selective dynein-mediated microtubule minus end-directed transport. *EMBO J.* **22,** 6004–6015 CrossRef Medline
125. Dienstbier, M., and Li, X. (2009) Bicaudal-D and its role in cargo sorting by microtubule-based motors. *Biochem. Soc. Trans.* **37,** 1066–1071 CrossRef Medline
126. Liu, Y., Salter, H. K., Holding, A. N., Johnson, C. M., Stephens, E., Lukavsky, P. J., Walshaw, J., and Bullock, S. L. (2013) Bicaudal-D uses a parallel, homodimeric coiled coil with heterotypic registry to coordinate recruitment of cargos to dynein. *Genes Dev.* **27,** 1233–1246 CrossRef Medline
127. Schlager, M. A., Serra-Marques, A., Grigoriev, I., Gumy, L. F., Esteves da Silva, M., Wulf, P. S., Akhmanova, A., and Hoogenraad, C. C. (2014) Bicaudal d family adaptor proteins control the velocity of dynein-based movements. *Cell Rep.* **8,** 1248–1256 CrossRef Medline
128. Schroeder, C. M., and Vale, R. D. (2016) Assembly and activation of dynein–dynactin by the cargo adaptor protein Hook3. *J. Cell Biol.* **214,** 309–318 CrossRef Medline
129. Olenick, M. A., Tokito, M., Boczkowska, M., Dominguez, R., and Holzbaur, E. L. (2016) Hook adaptors induce unidirectional processive motility by enhancing the dynein–dynactin interaction. *J. Biol. Chem.* **291,** 18239–18251 CrossRef Medline
130. Grotjahn, D. A., Chowdhury, S., Xu, Y., McKenney, R. J., Schroer, T. A., and Lander, G. C. (2018) Cryo-electron tomography reveals that dynactin recruits a team of dyneins for processive motility. *Nat. Struct. Mol. Biol.* **25,** 203–207 CrossRef Medline
131. Urnavicius, L., Lau, C. K., Elshenawy, M. M., Morales-Rios, E., Motz, C., Yildiz, A., and Carter, A. P. (2018) Cryo-EM shows how dynactin recruits two dyneins for faster movement. *Nature* **554,** 202–206 CrossRef Medline
132. Rai, A. K., Rai, A., Ramaiya, A. J., Jha, R., and Mallik, R. (2013) Molecular adaptations allow dynein to generate large collective forces inside cells. *Cell* **152,** 172–182 CrossRef Medline
133. Rai, A., Pathak, D., Thakur, S., Singh, S., Dubey, A. K., and Mallik, R. (2016) Dynein clusters into lipid microdomains on phagosomes to drive rapid transport toward lysosomes. *Cell* **164,** 722–734 CrossRef Medline
134. Wang, Z., and Sheetz, M. P. (2000) The C terminus of tubulin increases cytoplasmic dynein and kinesin processivity. *Biophys. J.* **78,** 1955–1964 CrossRef Medline
135. McKenney, R. J., Huynh, W., Vale, R. D., and Sirajuddin, M. (2016) Tyrosination of α-tubulin controls the initiation of processive dynein–dynactin motility. *EMBO J.* **35,** 1175–1185 CrossRef Medline
136. Nirschl, J. J., Magiera, M. M., Lazarus, J. E., Janke, C., and Holzbaur, E. L. (2016) α-Tubulin tyrosination and CLIP-170 phosphorylation regulate the initiation of dynein-driven transport in neurons. *Cell Rep.* **14,** 2637–2652 CrossRef Medline
137. Kubo, T., Yanagisawa, H.-A., Yagi, T., Hirono, M., and Kamiya, R. (2010) Tubulin polyglutamylation regulates axonemal motility by modulating activities of inner-arm dyneins. *Curr. Biol.* **20,** 441–445 CrossRef Medline
138. Suryavanshi, S., Eddé, B., Fox, L. A., Guerrero, S., Hard, R., Hennessey, T., Kabi, A., Malison, D., Pennock, D., Sale, W. S., Wloga, D., and Gaertig, J. (2010) Tubulin glutamylation regulates ciliary motility by altering inner dynein arm activity. *Curr. Biol.* **20,** 435–440 CrossRef Medline
139. Alper, J. D., Decker, F., Agana, B., and Howard, J. (2014) The motility of axonemal dynein is regulated by the tubulin code. *Biophys. J.* **107,** 2872–2880 CrossRef Medline
140. Rigort, A., Bäuerlein, F. J., Villa, E., Eibauer, M., Laugks, T., Baumeister, W., and Plitzko, J. M. (2012) Focused ion beam micromachining of eukaryotic cells for cryoelectron tomography. *Proc. Natl. Acad. Sci. U.S.A.* **109,** 4449–4454 CrossRef Medline
141. Bleck, C. K., Merz, A., Gutierrez, M. G., Walther, P., Dubochet, J., Zuber, B., and Griffiths, G. (2010) Comparison of different methods for thin section EM analysis of *Mycobacterium smegmatis*. *J. Microsc.* **237,** 23–38 CrossRef Medline
142. Asano, S., Fukuda, Y., Beck, F., Aufderheide, A., Förster, F., Danev, R., and Baumeister, W. (2015) A molecular census of 26S proteasomes in intact neurons. *Science* **347,** 439–442 CrossRef Medline
143. Dai, W., Fu, C., Khant, H. A., Ludtke, S. J., Schmid, M. F., and Chiu, W. (2014) Zernike phase-contrast electron cryotomography applied to marine cyanobacteria infected with cyanophages. *Nat. Protoc.* **9,** 2630–2642 CrossRef Medline
144. Danev, R., Tegunov, D., and Baumeister, W. (2017) Using the Volta phase plate with defocus for cryo-EM single particle analysis. *Elife* **6,** e23006 CrossRef Medline
145. Mahamid, J., Pfeffer, S., Schaffer, M., Villa, E., Danev, R., Cuellar, L. K., Förster, F., Hyman, A. A., Plitzko, J. M., and Baumeister, W. (2016) Visualizing the molecular sociology at the HeLa cell nuclear periphery. *Science* **351,** 969–972 CrossRef Medline
146. King, S. M. (2018) Turning dyneins off bends cilia. *Cytoskeleton* **75,** 372–381 CrossRef Medline

Setting the dynein motor in motion: New insights from electron tomography

Danielle A. Grotjahn and Gabriel C. Lander

J. Biol. Chem. 2019, 294:13202-13217.
doi: 10.1074/jbc.REV119.003095 originally published online July 8, 2019